AD-A075 328 ARMY ENGINEER WATERWAYS EXPERIMENT STATION VICKSBURG--ETC F/G 13/13
SAVANNAH HARBOR INVESTIGATION AND MODEL STUDY; VOLUME IV. REANA--ETC(U)
SEP 79 C J HUVAL , R H MULTER , P K SENTER

UNCLASSIFIED WES-HL-TR-2-580-VOL-4 NL

| OF |
ADA
075328

END
DATE FILMED
11 -79
DDC

LEVEL

TECHNICAL REPORT 2-580

SAVANNAH HARBOR INVESTIGATION AND MODEL STUDY

Volume IV

REANALYSIS OF FRESHWATER CONTROL PLAN

Numerical Model Study

by

Carl J. Huval, Roger H. Multer, Paul K. Senter, Marden B. Boyd

Hydraulics Laboratory
U. S. Army Engineer Waterways Experiment Station
P. O. Box 631, Vicksburg, Miss. 39180

September 1979
Final Report

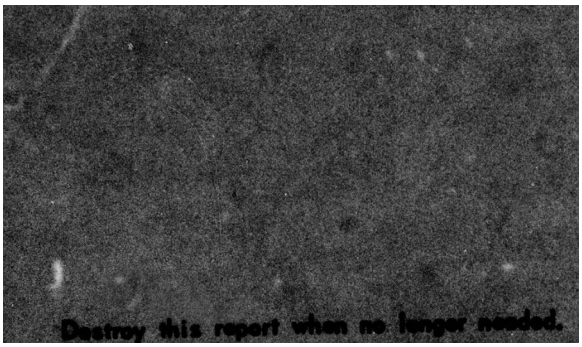
Destroy this report when no longer needed.

Unclassified

SECURITY CLASSIFICATION OF THIS PAGE (When Data Entered)

REPORT DOCUMENTATION PAGE

READ INSTRUCTIONS BEFORE COMPLETING FORM

1. REPORT NUMBER: Technical Report 2-580
2. GOVT ACCESSION NO.
3. RECIPIENT'S CATALOG NUMBER

4. TITLE (and Subtitle): SAVANNAH HARBOR INVESTIGATION AND MODEL STUDY; Volume IV, REANALYSIS OF FRESHWATER CONTROL PLAN, Numerical Model Study
5. TYPE OF REPORT & PERIOD COVERED: Final report, Dec 72-Apr 74,
6. PERFORMING ORG. REPORT NUMBER

7. AUTHOR(s): Carl J. Huval, Paul K. Senter, Roger H. Multer, Marden B. Boyd
8. CONTRACT OR GRANT NUMBER(s)

9. PERFORMING ORGANIZATION NAME AND ADDRESS: U. S. Army Engineer Waterways Experiment Station, Hydraulics Laboratory, P. O. Box 631, Vicksburg, Miss. 39180
10. PROGRAM ELEMENT, PROJECT, TASK AREA & WORK UNIT NUMBERS: 12 62

11. CONTROLLING OFFICE NAME AND ADDRESS: U. S. Army Engineer District, Savannah, P. O. Box 889, Savannah, Georgia 31402
12. REPORT DATE: Sep 1979
13. NUMBER OF PAGES: 57

14. MONITORING AGENCY NAME & ADDRESS (if different from Controlling Office): WES-HL-TR-2-580-VOL-4
15. SECURITY CLASS. (of this report): Unclassified
15a. DECLASSIFICATION/DOWNGRADING SCHEDULE

16. DISTRIBUTION STATEMENT (of this Report)

Approved for public release; distribution unlimited.

17. DISTRIBUTION STATEMENT (of the abstract entered in Block 20, if different from Report)

18. SUPPLEMENTARY NOTES

19. KEY WORDS (Continue on reverse side if necessary and identify by block number)

Environmental effects
Fresh water
Mathematical models
Salinity
Salt water intrusion
Savannah Harbor

20. ABSTRACT (Continue on reverse side if necessary and identify by block number)

An extensive series of physical model investigations was conducted during the late 1950's and early 1960's to develop plans for reducing maintenance dredging costs for Savannah Harbor. The plan developed involved dredging a sediment basin at the lower end of Back River, construction of a tide gate in Back River, dredging a connecting canal between Back River and Middle River, and channel improvements in the upstream portion of Back River. As the plan was being implemented, questions arose that required a reanalysis of the impact

(Continued)

CONT'

DD FORM 1 JAN 73 1473 EDITION OF 1 NOV 65 IS OBSOLETE

Unclassified

SECURITY CLASSIFICATION OF THIS PAGE (When Data Entered)

20. ABSTRACT (Continued).

CONT

of the plan on salinities in Little Back River. Numerical models, flow and salinity, were developed and applied to the channel network above Fort Jackson to estimate salinity levels at the location of the freshwater intake for the wildlife refuge adjacent to Little Back River. Computations for preproject conditions and with the plan fully implemented indicated relatively small salinity increases at the location of the intake. The computations also indicated that should these small increases prove detrimental, further improvements in the back channels could increase the freshwater inflow to the back channels. Appendices A and B of the report discuss the hydrodynamic and salinity models, respectively, used in the investigation.

PREFACE

The work described herein was conducted during the period December 1972 to April 1974 for the U. S. Army Engineer District, Savannah, by the U. S. Army Engineer Waterways Experiment Station (WES) under the general supervision of Messrs. H. B. Simmons, Chief of the Hydraulics Laboratory, and M. B. Boyd, Chief of the Mathematical Hydraulics Division (MHD). A preliminary report presenting most of the results and conclusions developed during the study was submitted to the District in August 1973. This final report was prepared during the period August-September 1978.

Mr. C. J. Huval, MHD, served as coordinator of the project and prepared the preliminary report. Dr. R. H. Multer, MHD, developed the numerical models used in the study and prepared the technical appendices contained in this report. Mr. P. K. Senter, Automatic Data Processing Center, programmed the computer models and aided in the testing program. Mr. Boyd developed this report based on material available from the preliminary report and subsequent documentation of tests run after the preliminary report was submitted.

Commanders and Directors of WES during the conduct of this study and the preparation and publication of this report were BG E. D. Peixotto, CE; COL G. H. Hilt, CE; COL John L. Cannon, CE; and COL Nelson P. Conover, CE. Technical Director was Mr. F. R. Brown.

CONTENTS

CONVERSION FACTORS, U. S. CUSTOMARY TO METRIC (SI) UNITS OF MEASUREMENT

U. S. customary units of measurement used in this report can be converted to metric (SI) units as follow:

Multiply	By	To Obtain
cubic feet per second	0.02831685	cubic metres per second
feet	0.3048	metres
feet per second	0.3048	metres per second
feet per second per second	0.3048	metres per second per second
miles (U. S. statute)	1.609344	kilometres
square feet	0.09290304	square metres

SAVANNAH HARBOR INVESTIGATION AND MODEL STUDY

REANALYSIS OF FRESHWATER CONTROL PLAN

Numerical Model Study

PART I: INTRODUCTION

Description and Background

1. Savannah Harbor is located on the South Atlantic coast, partly in South Carolina and partly in Georgia. The harbor is formed by the lower 31 miles* of the Savannah River, including a bar channel extending to the 36-ft contour in the Atlantic Ocean. The Savannah River's headwater tributaries rise in the Blue Ridge Mountains of North Carolina and unite to form the main stream which flows 297 miles to the city of Savannah. The Savannah River is tidal for approximately 50 miles, from its mouth to Ebenezer Landing (Plate 1).

2. A deep-draft navigation project extends up Front River to a point just downstream from the Coastal Highway Bridge. Maintenance of project depths has required considerable dredging, with the greater portion being required in the lower 4 miles of Front River since this reach encompasses the nodal point for predominance of bottom currents under conditions of normal freshwater discharge. As a result of these significant maintenance problems, an extensive series of physical model investigations was conducted during the latter half of the 1950's and early 1960's to develop plans for reducing maintenance dredging costs for Savannah Harbor.**

---

* A table of factors for converting U. S. customary units of measurement to metric (SI) units is presented on page 3.

** U. S. Army Engineer Waterways Experiment Station, CE. "Savannah Harbor Investigation and Model Study: Volume III, Results of Model Investigations," Technical Report No. 2-580, Vicksburg, Miss.

a. 1961. "Section 1, Model Verification and Results of General Studies."

b. 1961. "Section 2, Tests of Improvement Plans."

c. 1963. "Section 3, Results of Supplemental Tests."

d. H. J. Rhodes and H. B. Simmons. 1965. "Section 4, Results of Tests of Increased Channel Dimensions."

3. The major elements of the sediment basin-tide gate plan developed in the physical model investigations involve dredging a sediment basin at the lower end of Back River, construction of a tide gate in Back River, dredging a connecting canal between Back River and Middle River, and channel improvements through McCoombs Cut and into the upstream portion of Back River (Plate 2). The concept of the plan is for the tide gate structure to be open during the flood portion of the tidal cycle and then closed at high-water slack. This will cause major flow distribution changes in the lower channel complex since the tidal prism in the Back and Middle River areas must be drained through the Front River portion of the system. The higher ebb velocities resulting in Front River will tend to move the sediment on through the critical reach and concentrate much of the shoaling in the sediment basin at the lower end of Back River. This will permit more efficient dredging and disposal of the material.

4. The improved diversion channels through McCoombs Cut and the upper end of Little Back River were proposed to ensure fresh water for the Savannah Wildlife Refuge by maintaining salinities at the inlet structure in Little Back River at near preproject levels. The proposed flow diversion channels and improvements are shown in Plate 3. The intake to the freshwater supply canal system that will feed the wildlife refuge and some private hunting lands is sized to supply 300 cfs for inundation of the area during the fall. The channel improvements were designed for a freshwater inflow of 4000 cfs from Savannah River into the back channels (2500 cfs into Little Back River and 1500 cfs into Middle River) assuming steady-flow conditions and known channel bottom slopes. The impact on salinities in Little Back River was checked in the physical model study by pumping the design discharges from the Savannah River into Little Back and Middle Rivers (i.e., actual dynamic tests of the proposed channel enlargements were not conducted in the physical model). For the 4000-cfs freshwater diversion, salinities near the freshwater intake for the wildlife refuge were not significantly altered by the sediment trap plan.

The Problem

5. During 1972, as the U. S. Army Engineer District, Savannah, developed detail plans for a new freshwater intake at the wildlife refuge, questions were raised concerning the effectiveness of the proposed channel improvements in providing the required fresh water in Little Back River. A reevaluation of the complex unsteady-flow situation that exists in the upstream end of the channel network near McCoombs Cut caused concern that net flows of the design magnitudes would not be diverted from Savannah River into the back channels. At a conference involving personnel from the Savannah District; U. S. Army Engineer Division, South Atlantic; Office, Chief of Engineers; and the U. S. Army Engineer Waterways Experiment Station (WES), it was decided that additional studies of this situation should be made giving full consideration to the unsteady-flow conditions which exist in the upper channel complex and their impact on salinities at the location of the proposed freshwater intake.

Purpose and Scope of Study

6. The study reported herein was undertaken to provide more reliable information concerning flow and salinity changes in the Little Back River resulting from implementation of the sediment basin-tide gate plan. In order to provide this information, numerical models were developed to (a) calculate unsteady flows in a complex network of channels and (b) estimate time varying salinities throughout the system. Following model development, tests were run to determine the change in flows and salinities resulting from various stages of development of the sediment basin-tide gate plan.

7. Since the Savannah District was almost ready to let a contract for construction of a new freshwater intake at the wildlife refuge, preliminary results from this study were summarized in an interim report submitted to the district in August 1973. This report documents more fully the models developed, tests conducted, and results obtained.

PART II: THE NUMERICAL MODELS

Hydrodynamic Model

8. The portion of the Savannah Estuary of interest in this study includes a network of channels as shown in Plates 1 and 2. Some vertical stratification existed in the channel system, primarily in the navigation channel reach of Front River. However, this study was conducted on the assumption that a one-dimensional calculation (i.e. well-mixed system) would produce reliable indications of the impact of the plan. An unsteady-flow model capable of treating the Savannah Estuary Channel network (or other channel networks) was developed for this study. The one-dimensional unsteady-flow equations that formed the basis for this model are

$$\frac{\partial Q}{\partial t} + \frac{\partial}{\partial x} uQ + gA \frac{\partial \eta}{\partial x} + g \frac{Q|Q|}{AC^2R} = 0 \qquad (1)$$

and

$$\frac{\partial A}{\partial t} + \frac{\partial Q}{\partial x} = 0 \qquad (2)$$

and represent, respectively, the conservation of longitudinal momentum and mass. In these equations

Q = discharge, cfs

t = time, sec

u = mean velocity, fps

x = distance along channel, ft

A = cross-sectional area, ft^2

g = acceleration due to gravity, ft/sec^2

η = water-surface elevation, ft

C = Chezy coefficient

R = hydraulic radius, ft

Along the interior portions of the various branches of the channel network these equations were integrated numerically using a

predictor-corrector technique. At the boundary points of the system and at the junctions of various branches, special treatment based on the conservation of mass was required. A more detailed discussion of the hydrodynamic model is presented in Appendix A.

Salinity Model

9. The one-dimensional equation for conservation of a conservative constituent is

$$\frac{\partial s}{\partial t} + u \frac{\partial s}{\partial x} = \frac{\partial}{\partial x} E \frac{\partial s}{\partial x} \qquad (3)$$

where

s = conservative constituent

u = longitudinal velocity, fps

E = dispersion coefficient

This equation was the basis of the salinity model. Again, the equation was numerically integrated with special treatment required at the junctions and boundary points. The time-varying flow field computed with the hydrodynamic model was used as input data to the salinity model. More detailed discussion of the rationale for the salinity model is presented in Appendix B.

Schematization of Channel Network

10. The Savannah Estuary Channel network between Fort Jackson just upstream from Elba Island and a point near Ebenezer Landing (Plate 1) was simulated in the model. The upstream limit of the model was beyond the point of tidal influence. The schematic network for preproject (1950) conditions is shown in Plate 4 and a similar network for planned conditions (sediment basin-tide gate plan fully implemented) is shown in Plate 5. Table 1 gives the lengths of each branch in the networks and the spatial increments (Δx) used in the numerical integration process. In addition to nodes at all channel junctions, nodes are used

at the upstream end of the navigation channel because of the large change in cross section and at the tide gate location because of the necessity for gate opening and closing simulation.

11. The channel cross-section data were developed from hydrographic charts available from the Savannah District for 1950 conditions. Channel modifications since 1950 have been substantial, and updated sections were obtained in most of the channel network to form another set of channel sections compatible with 1972 conditions. This data base reflects the sediment trap and the new drainage canal connecting Back and Front Rivers as well as the deepening and widening of the Front River navigation channel. Three typical channel cross sections are presented in Plate 6 to illustrate relative channel depths and widths. Both cross-section data bases consisted of a series of tables of channel widths versus elevations at 10 or less equal elevation intervals plus the elevation of the channel bottom. Plate 6 shows how a Front River cross section was divided into equidepth segments.

Model Calibration and Verification

12. Calibration of the hydrodynamic model was based on field data collected in July 1950. This is some of the data used in verifying the Savannah Harbor Physical Model* and was selected because it approximates the mean tide for the Savannah Estuary. The calibration runs were made using the measured tidal elevation time history at Fort Jackson as the downstream boundary condition and the flow near Ebenezer Landing as the upstream boundary conditions. Computed water-surface time histories were compared with measured elevations at the tide gage locations shown in Plate 4. Agreement was very good with elevations differing by less than 0.5 ft at all stations and with timing of high and low water also agreeing closely. Computed and measured elevations at Bird Refuge on Back River and the ACL Bridge in the Savannah River are presented in Plate 7 as examples. An effort was made to verify some tide height data obtained

---

* See footnote on page 4.

in September 1972 (after Back River was blocked with the cofferdam at the the location of the proposed gate). Agreement was not as good as expected, but it was later confirmed by the Savannah District that the gage zero at Fort Jackson (the downstream boundary for the numerical model) had shifted by about 0.2 ft. This is felt to be the primary reason for poor verification of the 1972 data. Other test runs were conducted of the tidal hydraulic model to ensure that the model was producing tidal elevation and velocity results consistent with prototype and physical model results. It was concluded after the several numerical experiments and verification tests that the mathematical model satisfactorily reproduced the system and produced consistent and reliable results.

13. Calibration of the salinity model was more difficult because of complexities related to numerically modeling the diffusion process and the relatively limited data available in the back channels. After model development and adjustment, model computations for preproject conditions with mean tide and normal freshwater inflows (about 7000 cfs) were in good agreement with the measured high-water slack salinity profile in Front River. In the calibration runs, the dispersion coefficient E was set to zero since the numerical dispersion introduced by the numerical integration procedure resulted in satisfactory agreement between computed and measured salinities. Checks with other available data also appeared reasonable and led to confidence that model calculations would provide reasonable estimates of salinities throughout the system for different stages of plan implementation and with the fully implemented plan. A more extensive salinity verification was not considered practical due to time limitations and the requirement for extensive field data in the channel network simulated by the model.

PART III: TEST PROGRAM AND RESULTS

Test Conditions

14. The model test program was designed to provide estimates of flow and salinity conditions at different stages of implementation of the sediment basin-tide gate plan. Test 1 represented preproject conditions and Test 2 represented the situation that existed at the time of the study (cofferdam blocking Back River at tide gate location and a connecting canal dredged between Back River and Middle River). Test 3 simulated the situation that would exist with the tide gate completed and operating without any channel improvements to McCoombs Cut and the upstream reach of Little Back River. The completed plan as proposed was simulated in Test 4.

15. The four test conditions cited above had been run at the time of the preliminary report. Subsequent to that report, two additional tests were run to verify that net downstream flows in Little Back River could be increased by additional changes in the back channels. Test 4A was a repeat of Test 4 except that the new connecting canal between Back River and Middle River was dredged to el -31 rather than el -9, as used in Test 4. Test 5 was run to determine if blocking Middle River near its upstream intersection with Back River would increase flow into Back River. Each test condition is briefly summarized in Table 2.

16. All tests were quasi-steady-state tests (i.e., repetitive tide and salinity at the downstream boundary with a constant upstream inflow) using the same upstream and downstream boundary conditions. The input tide at the downstream boundary of the system (Fort Jackson) was the mean tide used in the earlier physical model tests (Plate 8). A constant freshwater inflow of 7300 cfs was used as the upstream boundary condition in the Savannah River near Ebenezer Landing. Union Creek, which flows into McCoombs Cut, was assumed for this study to be a storage basin that fills and drains with a reflecting boundary. This is considered a reasonable assumption to provide comparative test results. In the salinity model, the input salinity at Fort Jackson (Plate 12) was

taken from field data near Elba Island on 20 July 1950 and represents an average over depth. The tidal conditions during that period approximated mean tide conditions.

Discussion of Results

Tests 1-4

17. The results of Tests 1-4 presented in this report and discussed in subsequent paragraphs differ slightly from those presented in the preliminary report furnished the Savannah District in August 1973. The differences result from the correction of two of the data points defining the mean tide curve at Fort Jackson that was used as the driving downstream boundary conditions for all tests. This correction smoothes out some local irregularities in the computed results and changes some of the numerical values cited but does not impact the conclusions presented in the preliminary report.

18. Computed tidal elevations at selected locations in the channel complex are presented in Plates 8 and 9. The impact of the different test conditions on tidal elevations at Bull Street on Front River is insignificant. Farther upstream on the main channel at ACL Bridge (just upstream from McCoombs Cut), the different test conditions do result in measurable changes in tidal range and phasing. However, the difference between Test 1 (preproject) and Test 4 (plan fully implemented) is quite small. At Bird Refuge on Back River the changes are more pronounced. Closing of Back River with the cofferdam in Test 2 and with the tide gate in Tests 3 and 4 delays the ebb portion of the cycle by about three quarters of an hour at this location. The phase shift results from the longer flow path required when Back River is blocked during ebb. With the plan fully implemented (Test 4), the flood portion of the tidal cycle at Bird Refuge is advanced by about 15 minutes as a result of faster tidal wave propagation through the improved channels. the plan also reduces the tidal range about 0.6 ft at Bird Refuge.

19. Discharges calculated through the tidal cycle at selected stations are plotted in Plates 10 and 11. Discharges through McCoombs Cut and at Bird Refuge on Back River (Plate 10) are important in

analyzing the effect of the plan on flow and salinity conditions in Back River and are summarized below:

Test Condition	McCoombs Cut		Bird Refuge on Back River	
	Peak D.S. Discharge cfs	Net D.S. Discharge cfs	Peak D.S. Discharge cfs	Net D.S. Discharge cfs
1	530	135	4160	190
2	1370	440	2920	300
3	1140	435	2850	75
4	3230	1350	3190	680

In Test 1 (preproject conditions) the net downstream flow at Bird Refuge is larger than the net flow through McCoombs Cut because there is a net upstream flow in Middle River. When compared with Test 1 discharges, Test 3 (before channel improvements in McCoombs Cut and upper Back River) results in some increase in flow through McCoombs Cut but decreases the net downstream flow at Bird Refuge on Back River. Improvement of the channels in the McCoombs Cut area (Test 4) approximately triples the net downstream discharge through McCoombs Cut and increases the net downstream discharge at Bird Refuge by a factor of about nine in comparison with computed discharges in Test 3. Computed discharges at Bull Street on Front River and at cross tides on Back River are plotted in Plate 11 to document the flow changes in other parts of the system.

20. Plates 12 and 13 present computed salinity variations through the tidal cycle at selected stations. High-water slack salinity profiles in Back River and Front River are shown in Plates 14 and 15, respectively. Operation of the tide gate structure in Test 3 increases the peak salinity at Bird Refuge on Back River to about 4.8 ppt. The proposed improvements in the channel through McCoombs Cut and in the upper end of Back River (Test 4) reduce the peak salinity to about 2.2 ppt. The computed peak salinity for preproject conditions (Test 1) was 0.9 at this location. The higher salinities in Back River with tide gate operation result from the trapping of more saline water in Back River when the tide gate is closed at high-water slack. The net effect of this is to transfer the salinity at the tide gate location

during the flood portion of the cycle (about 6 ppt) to the location of the new dredged canal connecting Back River with Middle River. How rapidly the salinities decrease upstream from that point on Back River depends upon the magnitude of the freshwater inflows into Back River. Study of the salinity profile in Plate 14 shows the effect of the changes in discharges in the back channels discussed in the preceding paragraph.

21. Salinity changes in Front River are less important but are worth noting (Plate 15). Implementation of the tide gate plan lowers the high-water slack salinity profile between Fort Jackson and Bull Street and significantly raises the profile from Bull Street to a point just upstream from the end of the navigation channel. Peak salinities at the Sugar Refinery location just upstream from the canal connection with Back River are increased from essentially zero for preproject conditions to about 2.5 ppt for the fully implemented plan (Plate 13).

22. Based on the results of these four tests, as reported in the preliminary report on the study, it was suggested that the Savannah District proceed with implementation of the plan as originally designed. This suggestion was based on the following rationale. While the net freshwater inflow into Back River was not as high as that originally estimated (computed at about 680 cfs compared with 2500 cfs used in an earlier physical model study), the calculations indicated that the peak salinity at Bird Refuge would only increase from about 0.9 ppt for preproject conditions to approximately 2.2 ppt with the fully implemented plan. No specific guidance had been provided concerning the acceptable peak salinity at Bird Refuge, but it was felt that the projected increase would probably not be objectionable. Also, should monitoring of the situation at Bird Refuge indicate the salinity increase to be detrimental, the situation can be reversed to essentially preproject conditions by leaving the tide gate open throughout the tidal cycle. This would provide a short-term solution and it was felt that further changes and/or improvements in the back channels could be made to increase the freshwater inflow into Back River. A short time after the preliminary report was prepared, the Savannah District authorized WES to make two additional runs to verify that larger freshwater flows in Back River

could be obtained if necessary. The results of these tests are briefly described in subsequent paragraphs.

Tests 4A and 5

23. A number of possible channel modifications which offer potential for increasing downstream net flow in Back River were considered:

a. Closing of Middle River in its upper reaches.

b. Closing of Middle River in its lower reaches.

c. Construction of a flow restriction in the upper reaches of Middle River.

d. Further extension of the channel modifications in Little Back River to Bird Refuge.

e. Channel improvements in the connection between Front and Back Rivers.

f. Modification in gate operation to reduce salinities such as gate closure for one or two tidal cycles per week.

Modifications e and a were selected for testing as Tests 4A and 5, respectively. Discharges calculated at McCoombs Cut and Bird Refuge throughout the tidal cycle are plotted in Plate 16 along with results from Test 4. Peak and net discharges are summarized below.

	McCoombs Cut		Bird Refuge on Back River	
Test Condition	Peak D.S. Discharge cfs	Net D.S. Discharge cfs	Peak D.S. Discharge cfs	Net D.S. Discharge cfs
4	3230	1350	3190	680
4A	3160	1540	3850	930
5	3095	890	3460	835

Deepening the connecting canal between Back River and Front River increased the net downstream discharge in McCoombs Cut and at Bird Refuge by about 15 and 35 percent, respectively. Blocking Middle River near the upstream end actually reduced net flow through McCoombs Cut but increased the net downstream flow in Back River by about 20 percent.

24. The impact of the increased net flow on peak salinity at Bird Refuge is indicated in the following tabulation.

Test Condition	Peak Salinity at Bird Refuge, ppt
4	2.2
4A	2.3
5	2.0

Blocking Middle River (Test 5) resulted in a small decrease in peak salinity to about 2.0 ppt. However, deepening the connecting canal between Back River and Middle River (Test 4A) resulted in a slight increase in peak salinity even though this change produced larger increases in net downstream flow at McCoombs Cut and Bird Refuge than the change made in Test 5. The slight increase in peak salinity is attributed to the longer period of flood currents into Back River which resulted with this test condition. These channel modifications had negligible effects on salinities in Front River.

25. Results of Tests 4A and 5 verify that, if necessary, additional channel modifications can be developed to increase freshwater flows into Back River. However, they also show that channel modifications must be carefully evaluated to ensure that the larger net flows in Back River also reduce peak salinities at Bird Refuge. No attempt was made to identify the optimum channel modification since the need for further modification has not been indicated.

PART IV: CONCLUSIONS AND RECOMMENDATIONS

26. The numerical calculations reported herein suggest the following conclusions and recommendations.

a. The net freshwater inflow into Back River with the sediment basin-tide gate plan fully implemented will not be as large as had earlier been estimated. The dynamic calculations indicate a net downstream flow of about 680 cfs compared with 2500 cfs used in the earlier physical model study.

b. Full implementation of the plan will cause a relatively small increase in peak salinities at Bird Refuge on Back River, from about 0.9 ppt for preproject conditions to approximately 2.2 ppt for the fully implemented plan.

c. Since no specific guidance is available concerning acceptable peak salinities, monitoring of salinity conditions at Bird Refuge is recommended as the plan is implemented. Should the relatively small salinity increase prove detrimental, the situation can be reversed to essentially preproject conditions by leaving the tide gate open throughout the tidal cycle. This type of operation would only be appropriate for short periods of time or until other modifications could be made since continuous operation with the tide gate open would make the sediment trap plan ineffective.

d. If necessary, the net downstream discharge in Back River could be increased by further modifications in the back channels. Two of the several possible channel changes were tested to verify that the net downstream flow could be increased, but no attempt was made to identify the optimum channel modification since the need for further modification has not been indicated.

Table 1

Total Branch and Incremental Lengths

Preproject (1950) Conditions			Present (1972) Conditions			Proposed Channel Improvements		
Branch No.	Length ft	Δx ft	Branch No.	Length ft	Δx ft	Branch No.	Length ft	Δx ft
			Changed Branches			Changed Branches		
1	6,700	1,675	3	23,200	2,700	10	4,800	960
2	45,600	2,682	4	5,280	1,760	16	44,460	2,340
3	86,800	2,553	5	7,500	1,500			
4	15,100	1,510	New Branches					
5	12,600	1,400						
6	8,000	1,600	13	12,765	2,553			
7	19,800	2,475	15	2,600	1,300			
8	17,400	1,933	16	50,540	2,660			
9	1,100	550	17	5,190	1,730			
10	6,100	1,220	18	9,810	1,635			
11	14,200	2,840						
12	114,655	4,985						

NOTE: ALL OTHER BRANCHES REMAINED AS THE 1950 CONFIGURATION.

Table 2

Test Conditions

Test No.	Channel Configuration	Gate	Diversion Channels	Notes
1	1950	None	Unimproved	Preproject
2	1972	Closed	Unimproved	Existing
3	1972	Operating	Unimproved	No dredging
4	1972	Operating	Improved	Planned conditions
4A	1972	Operating	Improved	Connecting canal between Back River and Middle River deepened
5	1972	Operating	Improved	Middle River blocked at upstream end

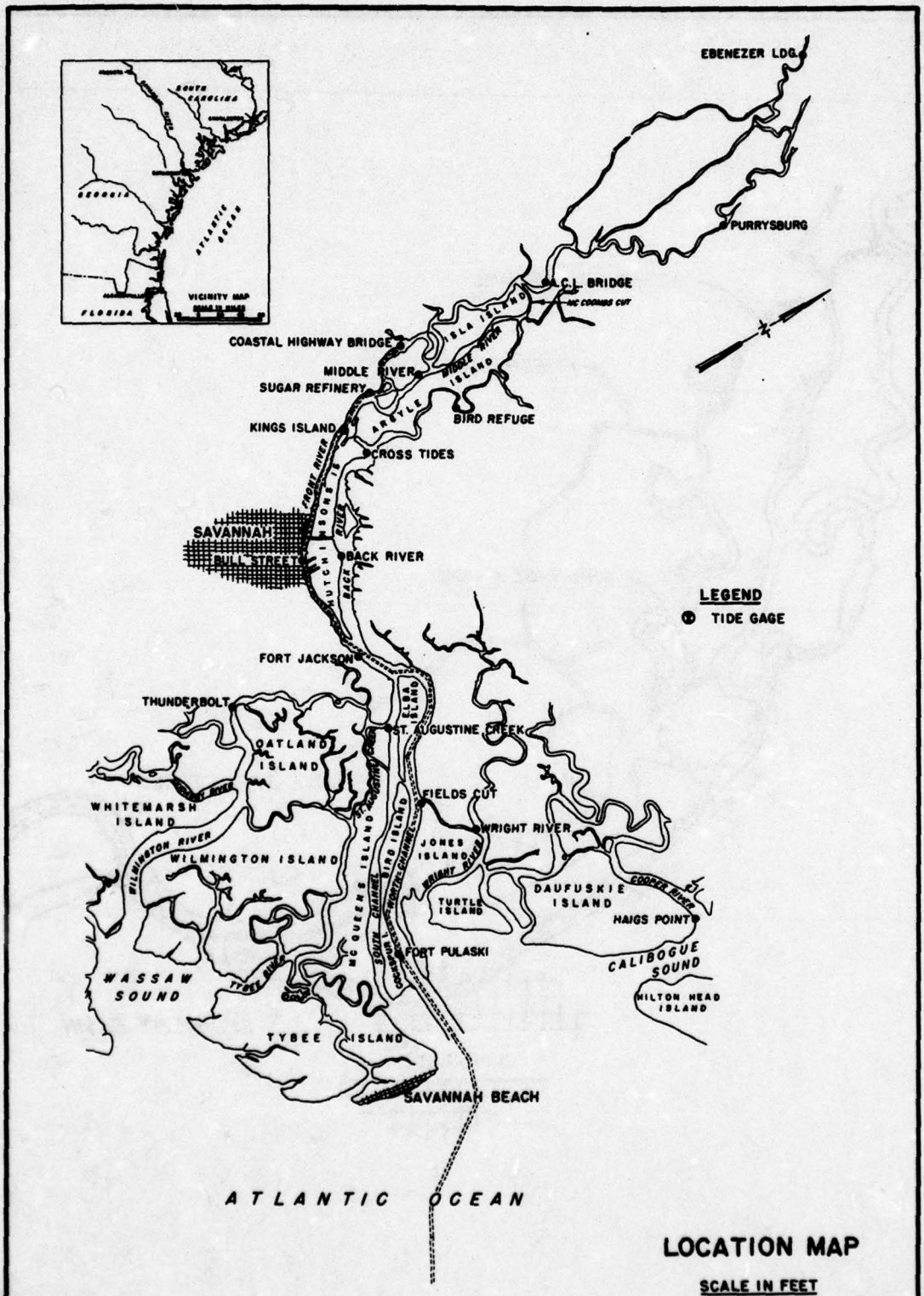

LOCATION MAP

SCALE IN FEET

PROTOTYPE 8000 0 8000 16000

PLATE 1

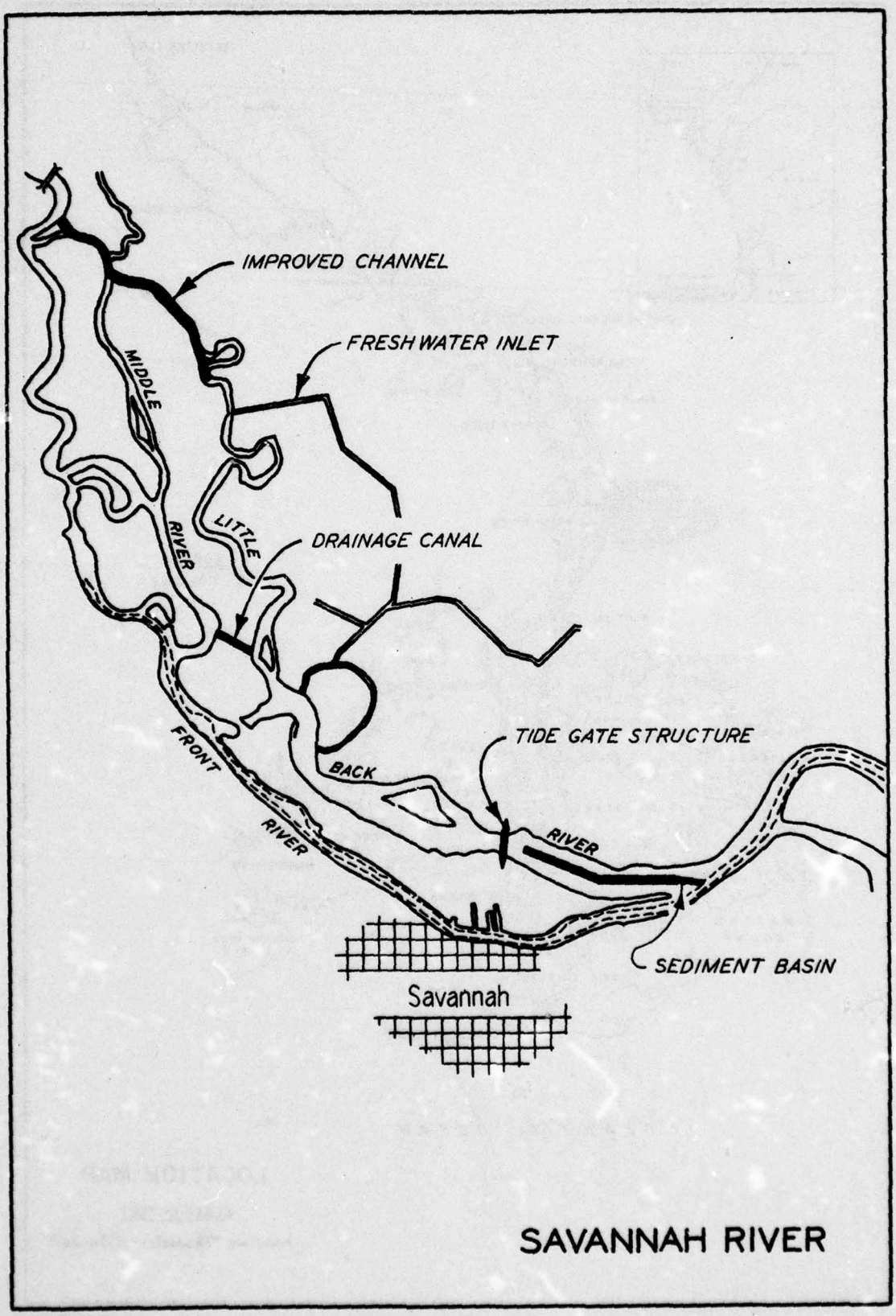
IMPROVED CHANNEL
FRESH WATER INLET
MIDDLE
RIVER
LITTLE
DRAINAGE CANAL
FRONT
RIVER
BACK
TIDE GATE STRUCTURE
RIVER
SEDIMENT BASIN
Savannah
SAVANNAH RIVER

PLATE 2

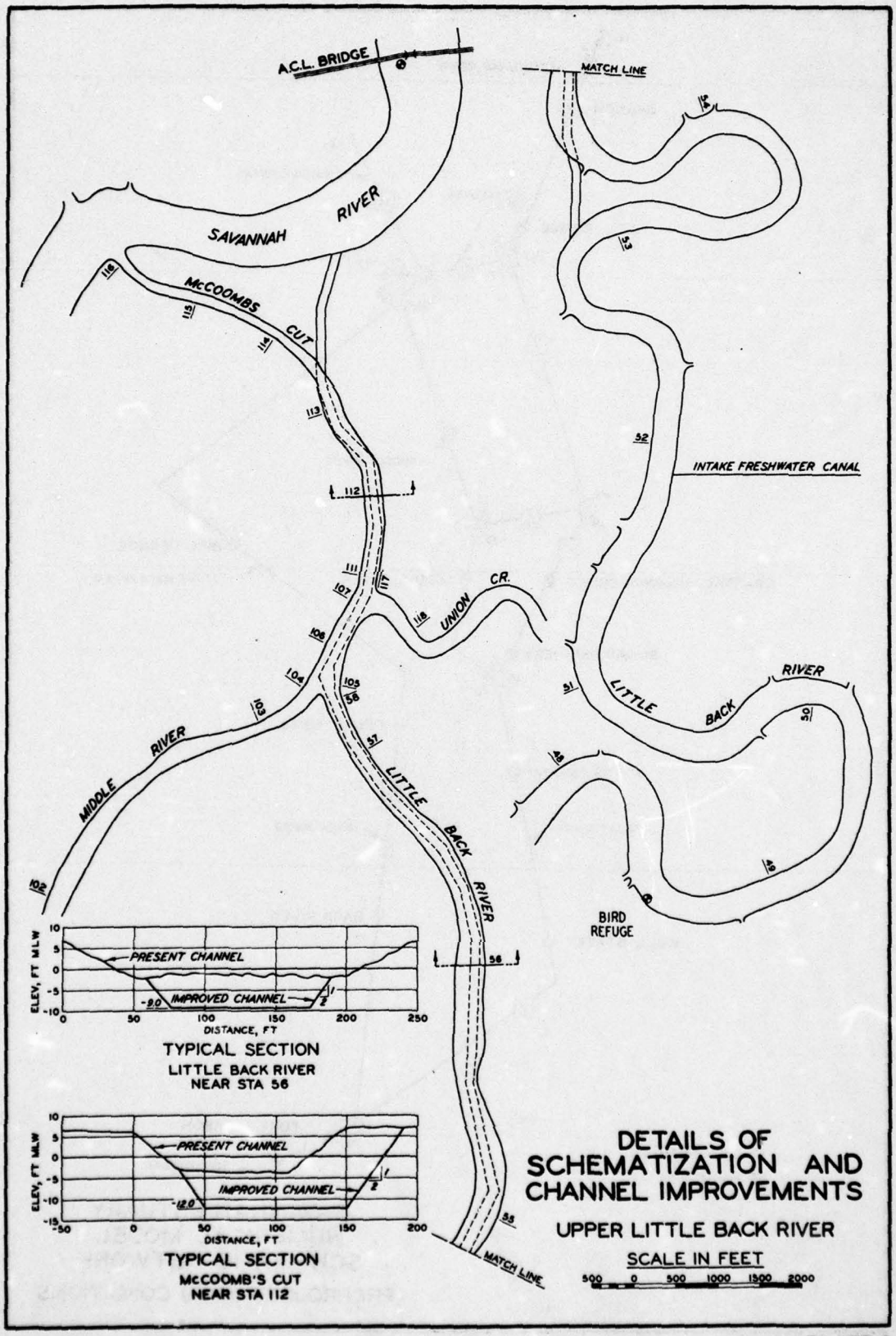
A.C.L. BRIDGE
MATCH LINE
SAVANNAH RIVER
McCOOMBS CUT
INTAKE FRESHWATER CANAL
UNION CR.
LITTLE BACK RIVER
MIDDLE RIVER
LITTLE BACK RIVER
BIRD REFUGE
MATCH LINE
ELEV, FT M.L.W
PRESENT CHANNEL
IMPROVED CHANNEL
-9.0
DISTANCE, FT
TYPICAL SECTION
LITTLE BACK RIVER
NEAR STA 56
ELEV, FT M.L.W
PRESENT CHANNEL
IMPROVED CHANNEL
-12.0
DISTANCE, FT
TYPICAL SECTION
McCOOMB'S CUT
NEAR STA 112
DETAILS OF SCHEMATIZATION AND CHANNEL IMPROVEMENTS
UPPER LITTLE BACK RIVER
SCALE IN FEET
500 0 500 1000 1500 2000

PLATE 3

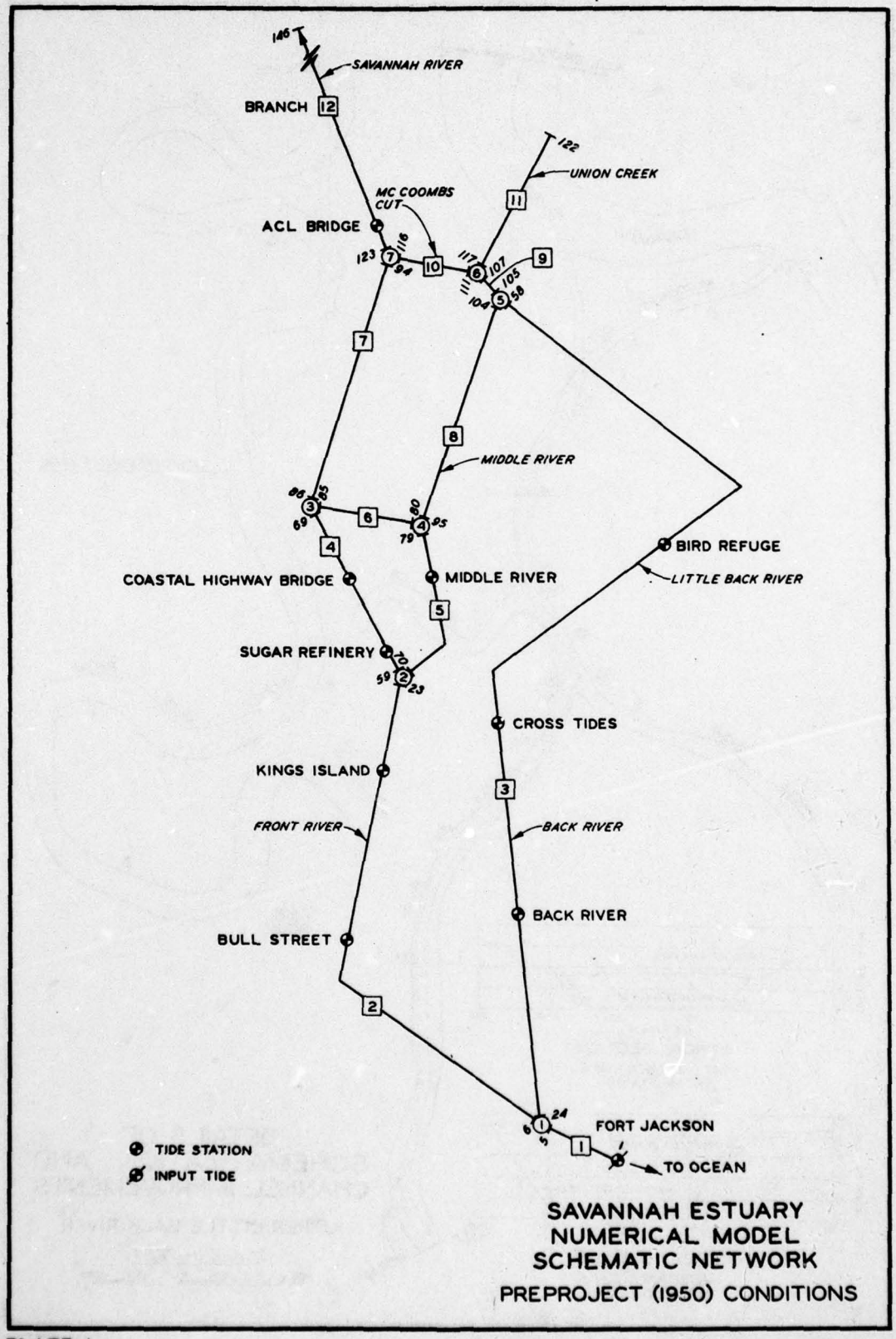

SAVANNAH ESTUARY
NUMERICAL MODEL
SCHEMATIC NETWORK
PREPROJECT (1950) CONDITIONS

PLATE 4

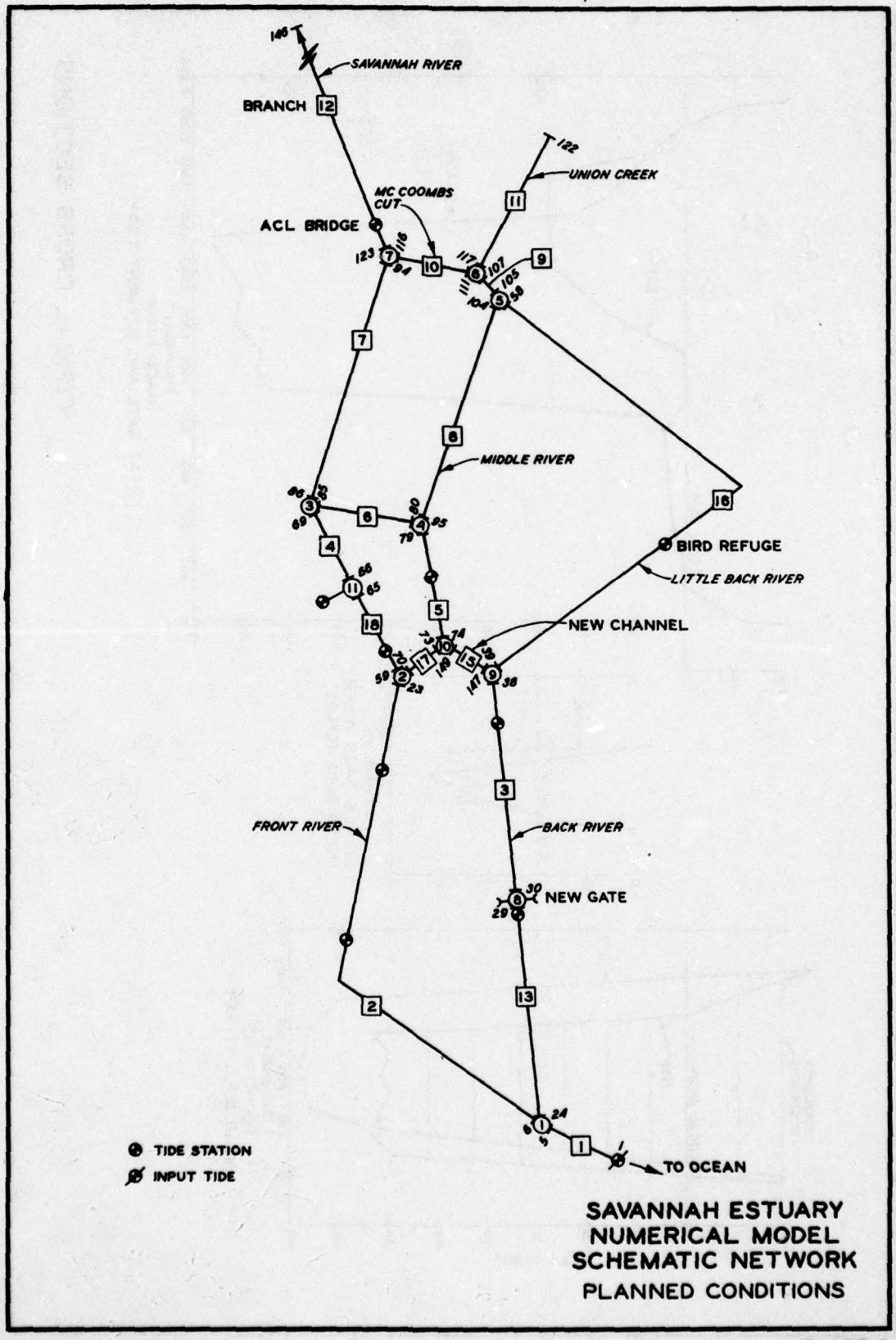

SAVANNAH ESTUARY
NUMERICAL MODEL
SCHEMATIC NETWORK
PLANNED CONDITIONS

PLATE 5

PLATE 6

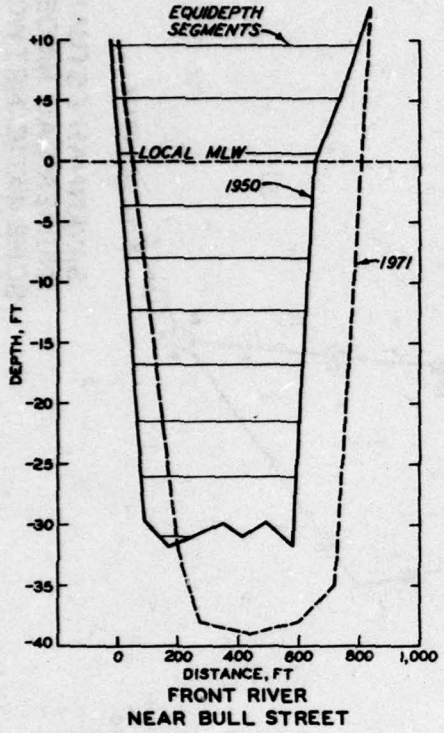

FRONT RIVER
NEAR BULL STREET

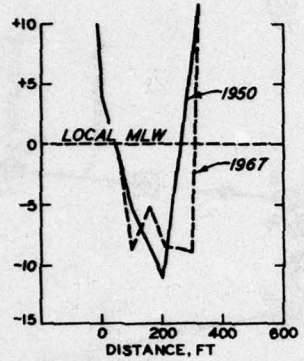

LITTLE BACK RIVER
NEAR BIRD REFUGE

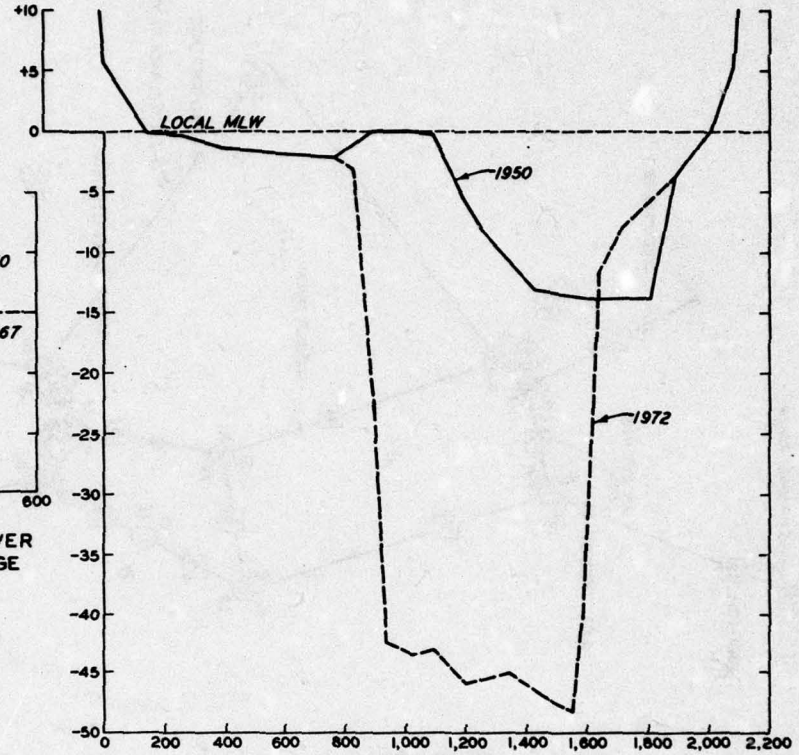

BACK RIVER
NEAR GATE AND SEDIMENT TRAP

TYPICAL CROSS SECTIONS

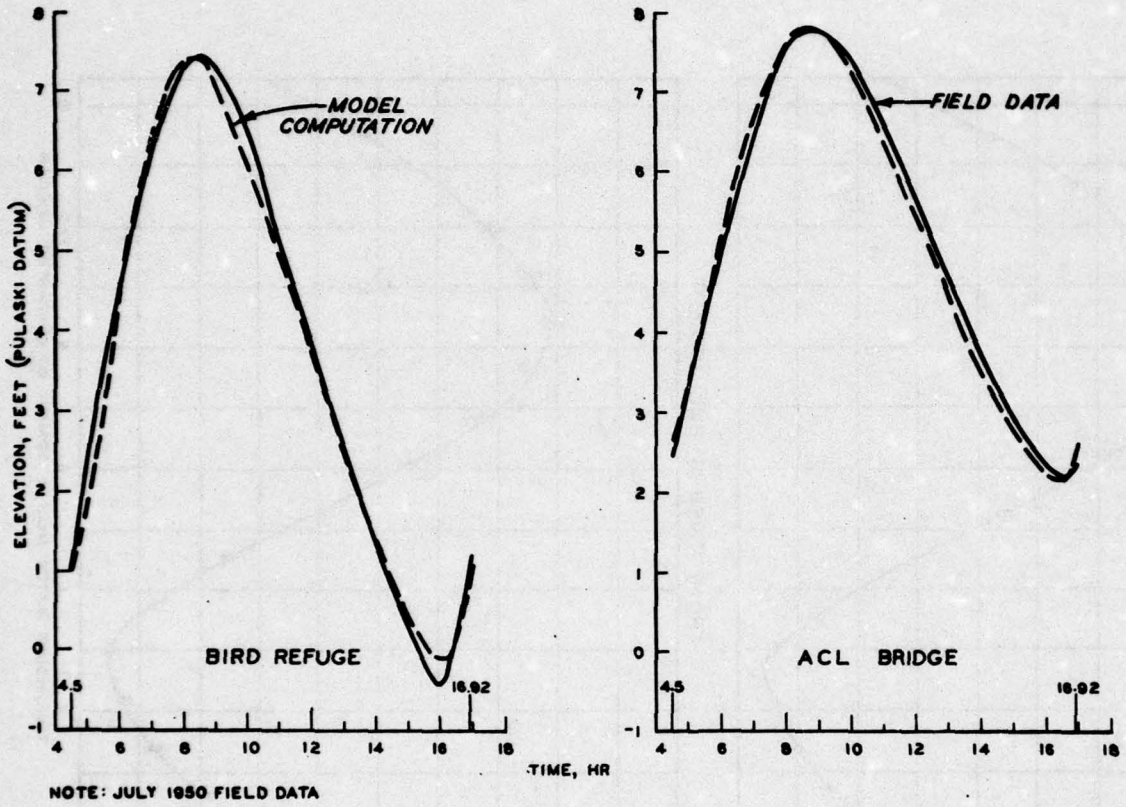

NOTE: JULY 1950 FIELD DATA

SAVANNAH ESTUARY
NUMERICAL MODEL
MODEL ADJUSTMENT

PLATE 7

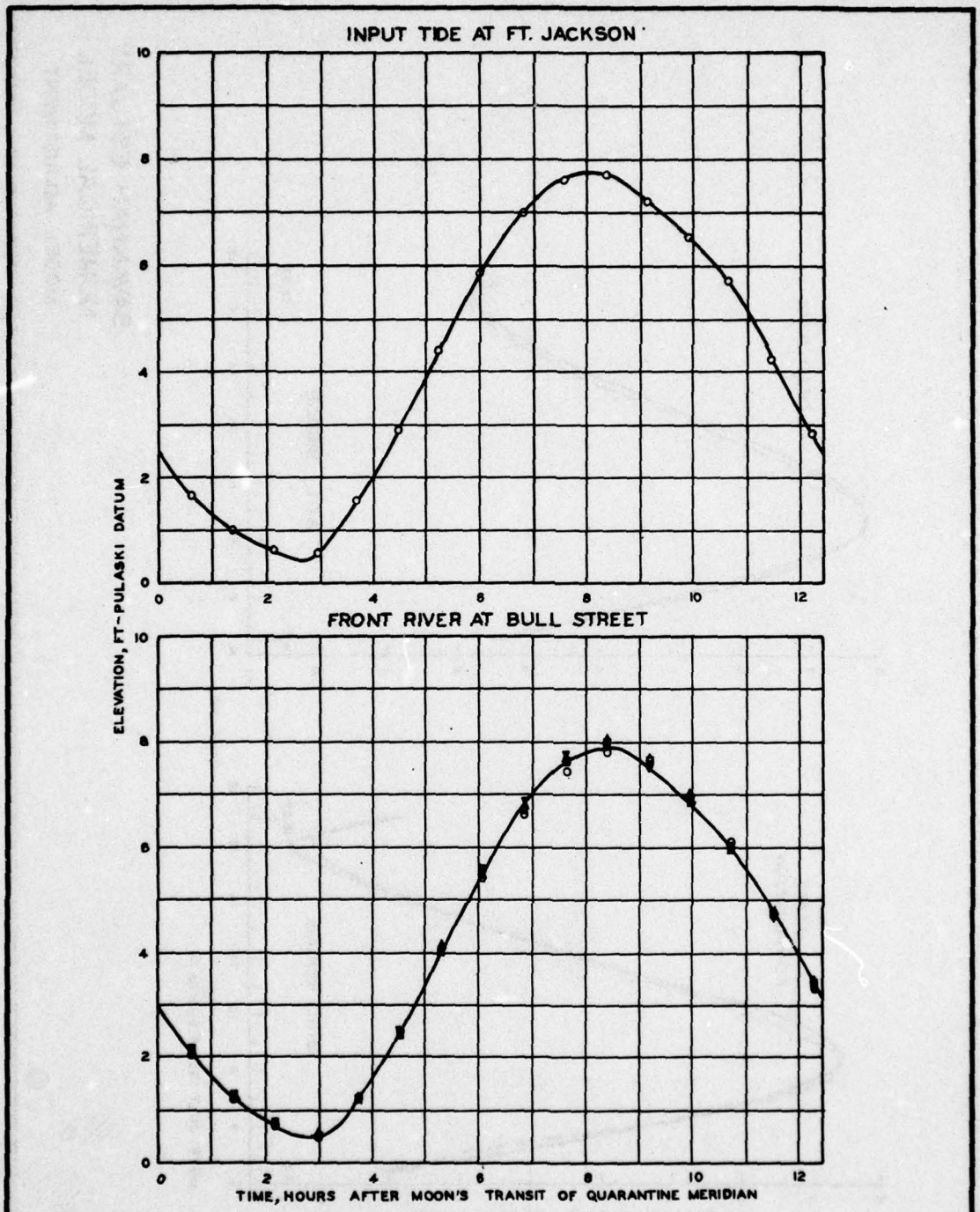

LEGEND

TEST NO.	SYMBOL
1	□
2	○
3	△
4	▽

TIDE.....MEAN
FRESHWATER DISCHARGE ..7300 CFS

TIDAL COMPUTATIONS

FT. JACKSON AND FRONT RIVER AT BULL STREET

PLATE 8

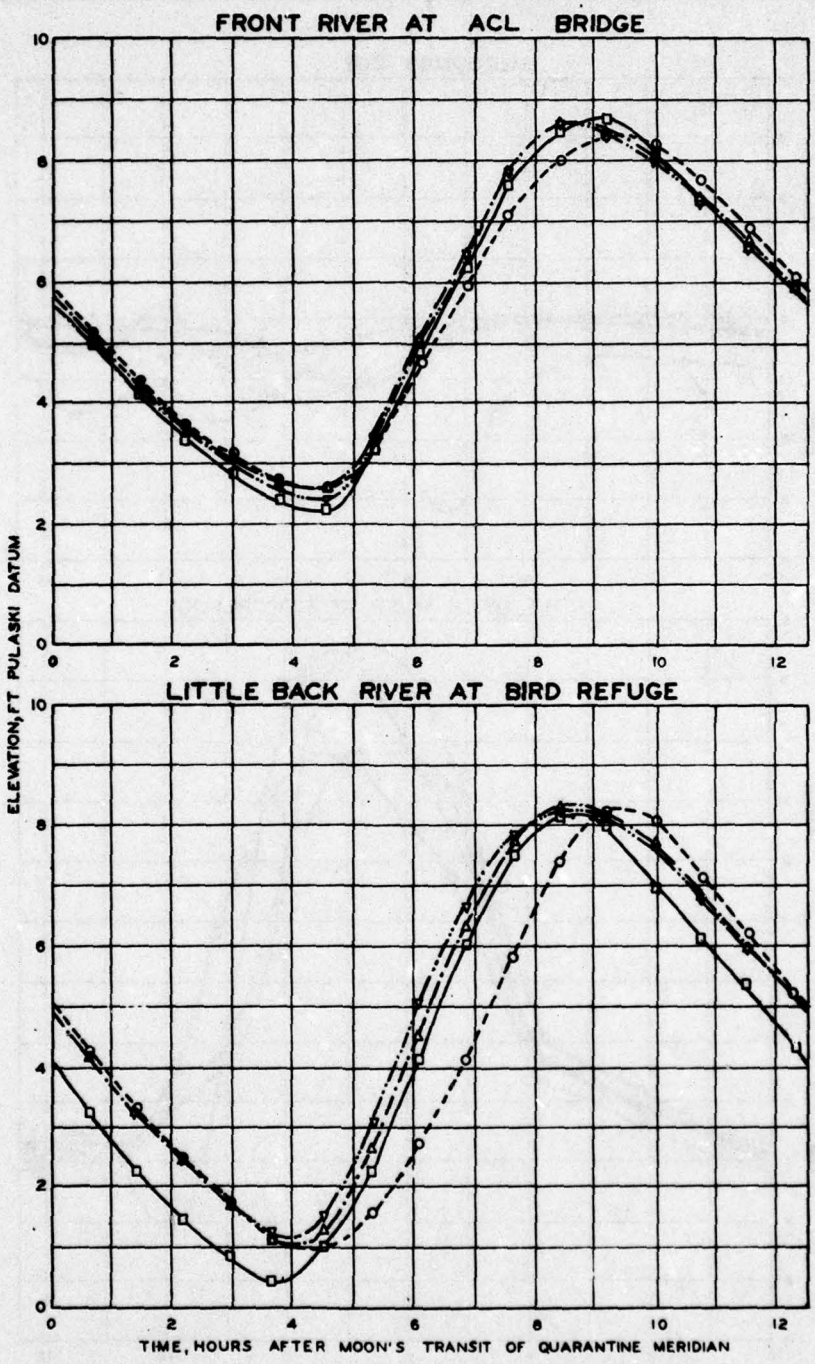

LEGEND

TEST NO.	SYMBOL
1	
2	
3	
4	

TIDE ..... MEAN
FRESHWATER DISCHARGE.. 7300 CFS

TIDAL COMPUTATIONS

FRONT RIVER AT ACL BRIDGE
AND LITTLE BACK RIVER
AT BIRD REFUGE

PLATE 9

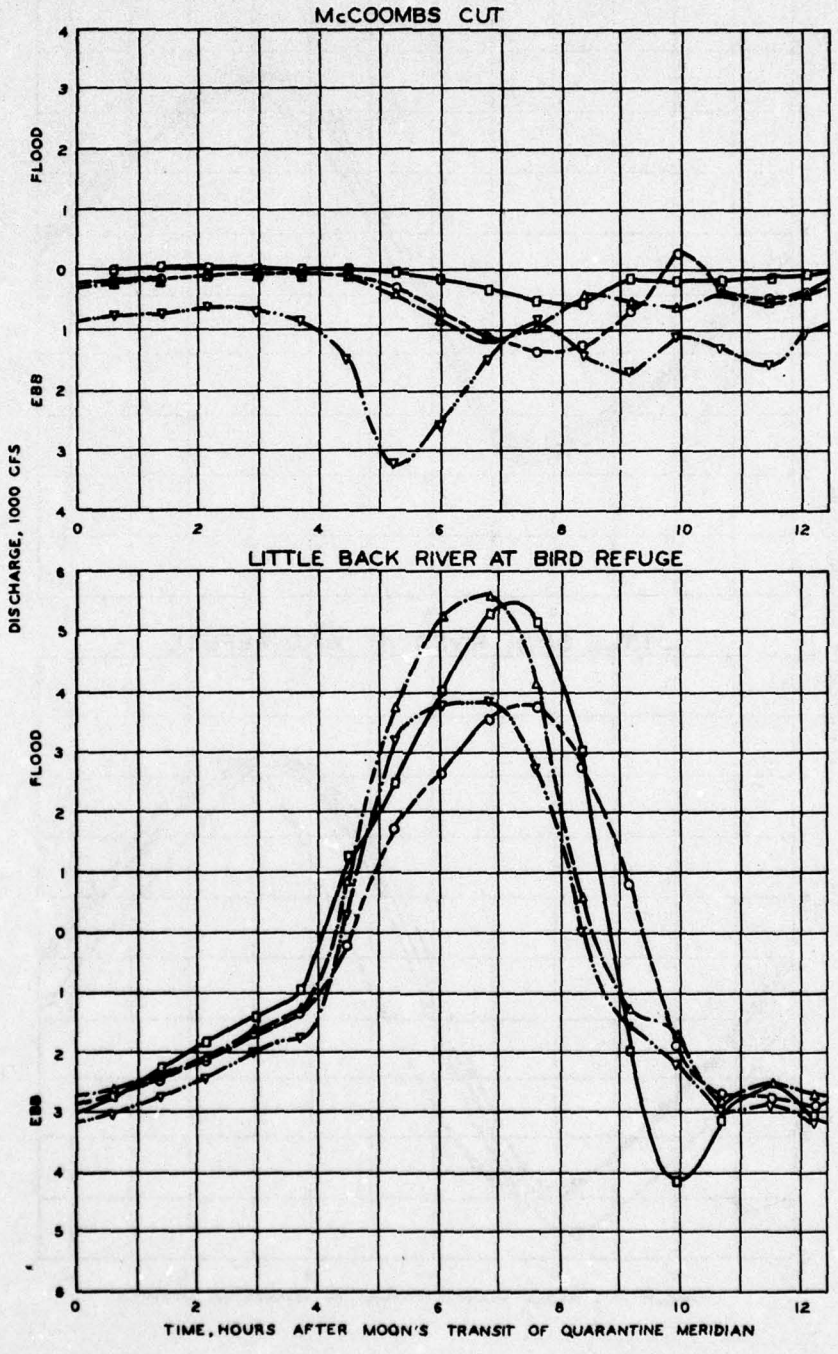

LEGEND

TEST NO.	SYMBOL
1	
2	
3	
4	

TIDE.....MEAN
FRESHWATER DISCHARGE...7300 CFS

DISCHARGE COMPUTATIONS
McCOOMBS CUT AND
LITTLE BACK RIVER AT BIRD REFUGE
TESTS 1-4

PLATE 10

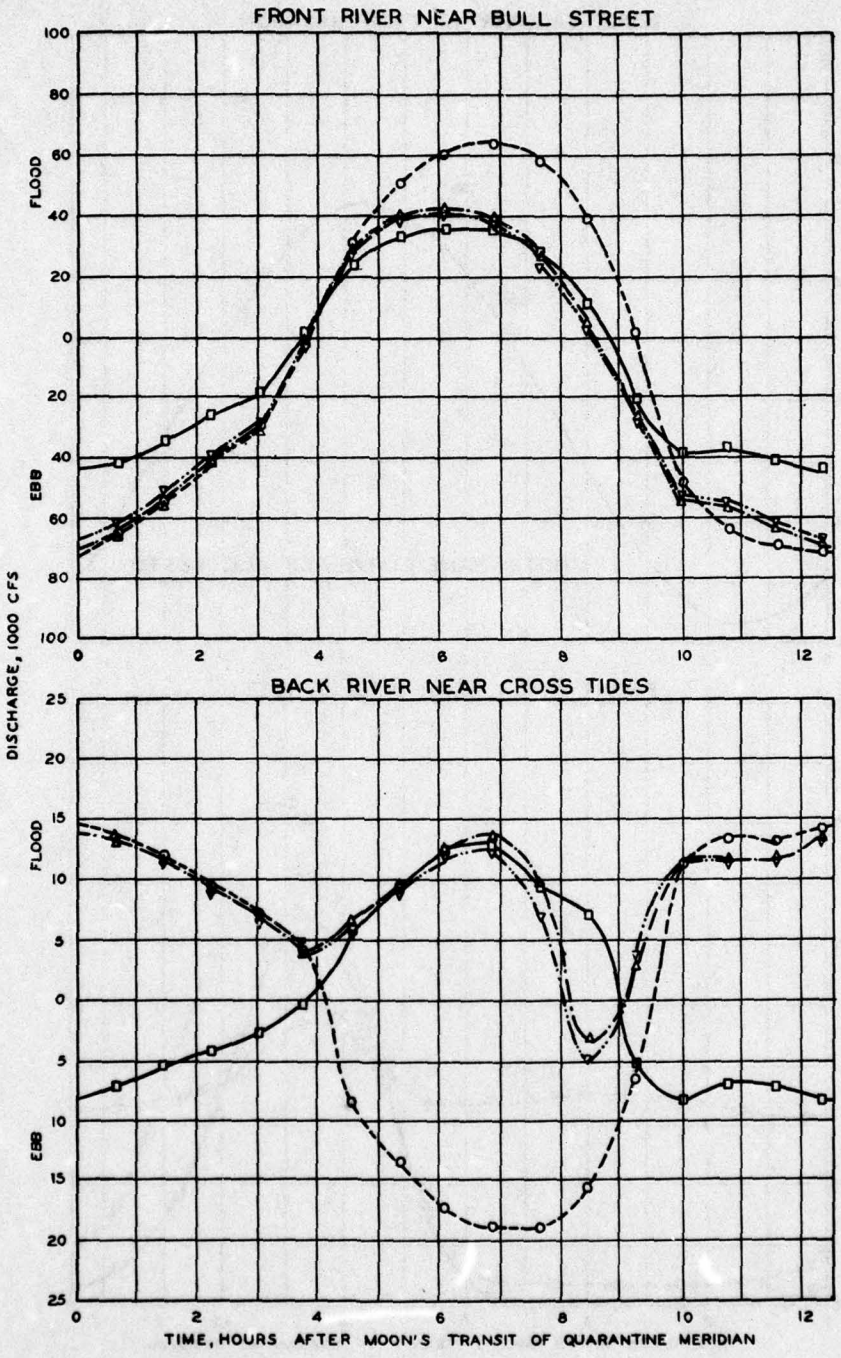

TIDE.....MEAN
FRESHWATER DISCHARGE..7300 CFS

LEGEND

TEST NO.	SYMBOL
1	
2	
3	
4	

DISCHARGE COMPUTATIONS

FRONT RIVER NEAR BULL STREET AND BACK RIVER NEAR CROSS TIDES

PLATE 11

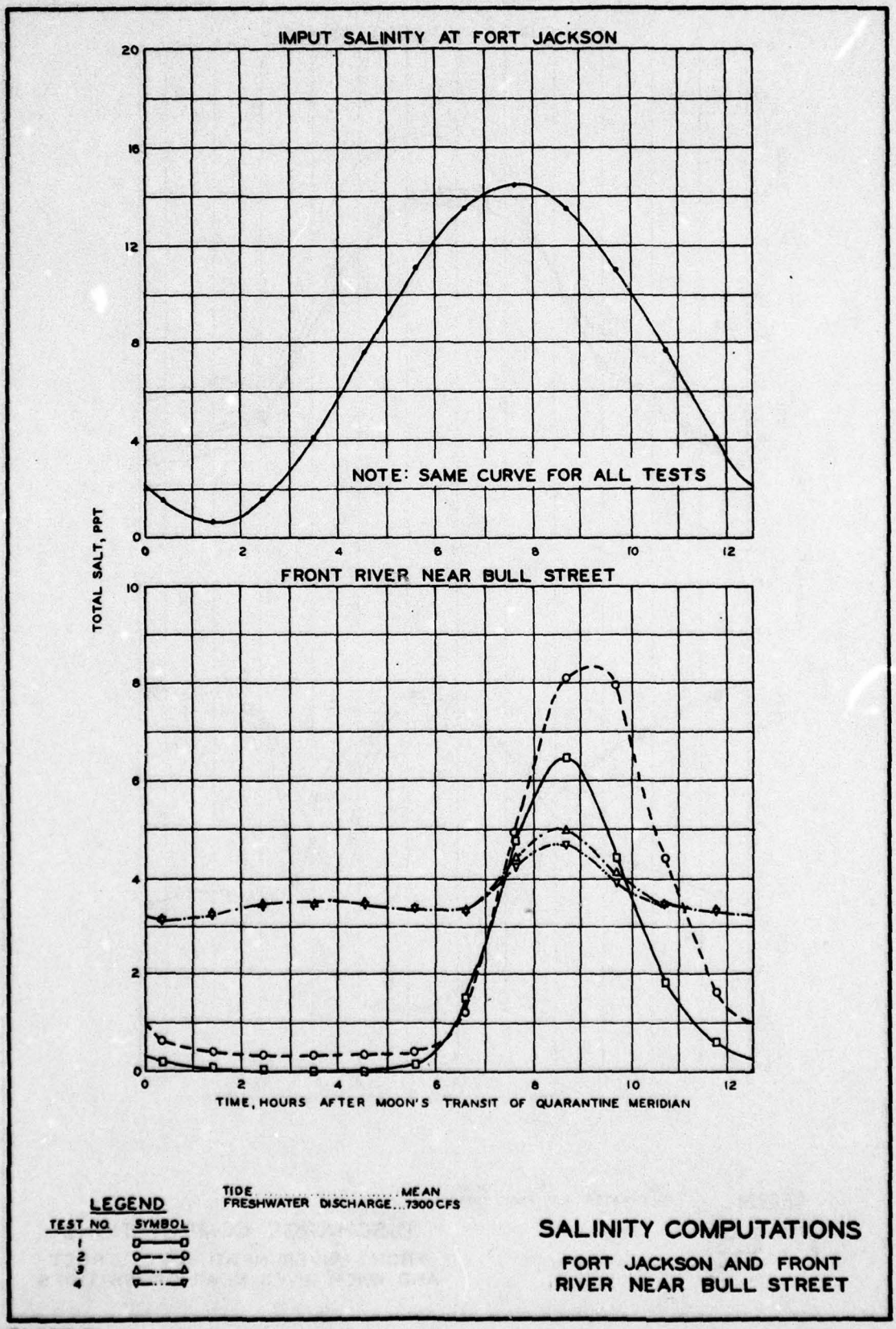
IMPUT SALINITY AT FORT JACKSON
NOTE: SAME CURVE FOR ALL TESTS
FRONT RIVER NEAR BULL STREET
TOTAL SALT, PPT
TIME, HOURS AFTER MOON'S TRANSIT OF QUARANTINE MERIDIAN
LEGEND
TEST NO. SYMBOL
1
2
3
4
TIDE ..... MEAN
FRESHWATER DISCHARGE...7300 CFS
SALINITY COMPUTATIONS
FORT JACKSON AND FRONT RIVER NEAR BULL STREET

PLATE 12

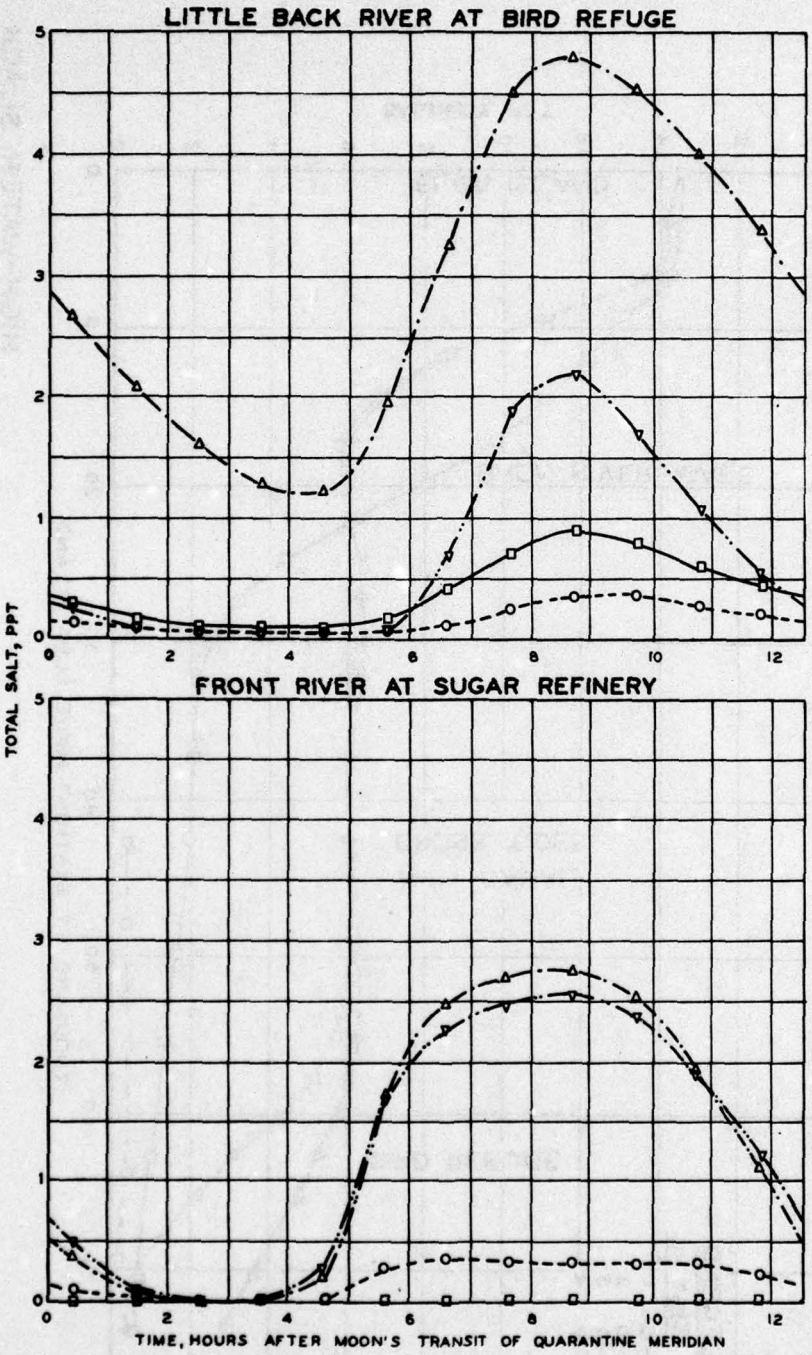

TIDE ..... MEAN
FRESHWATER DISCHARGE.. 7300 CFS

LEGEND

TEST NO.	SYMBOL
1	
2	
3	
4	

SALINITY COMPUTATIONS

LITTLE BACK RIVER AT BIRD REFUGE AND FRONT RIVER AT SUGAR REFINERY

PLATE 13

PLATE 14

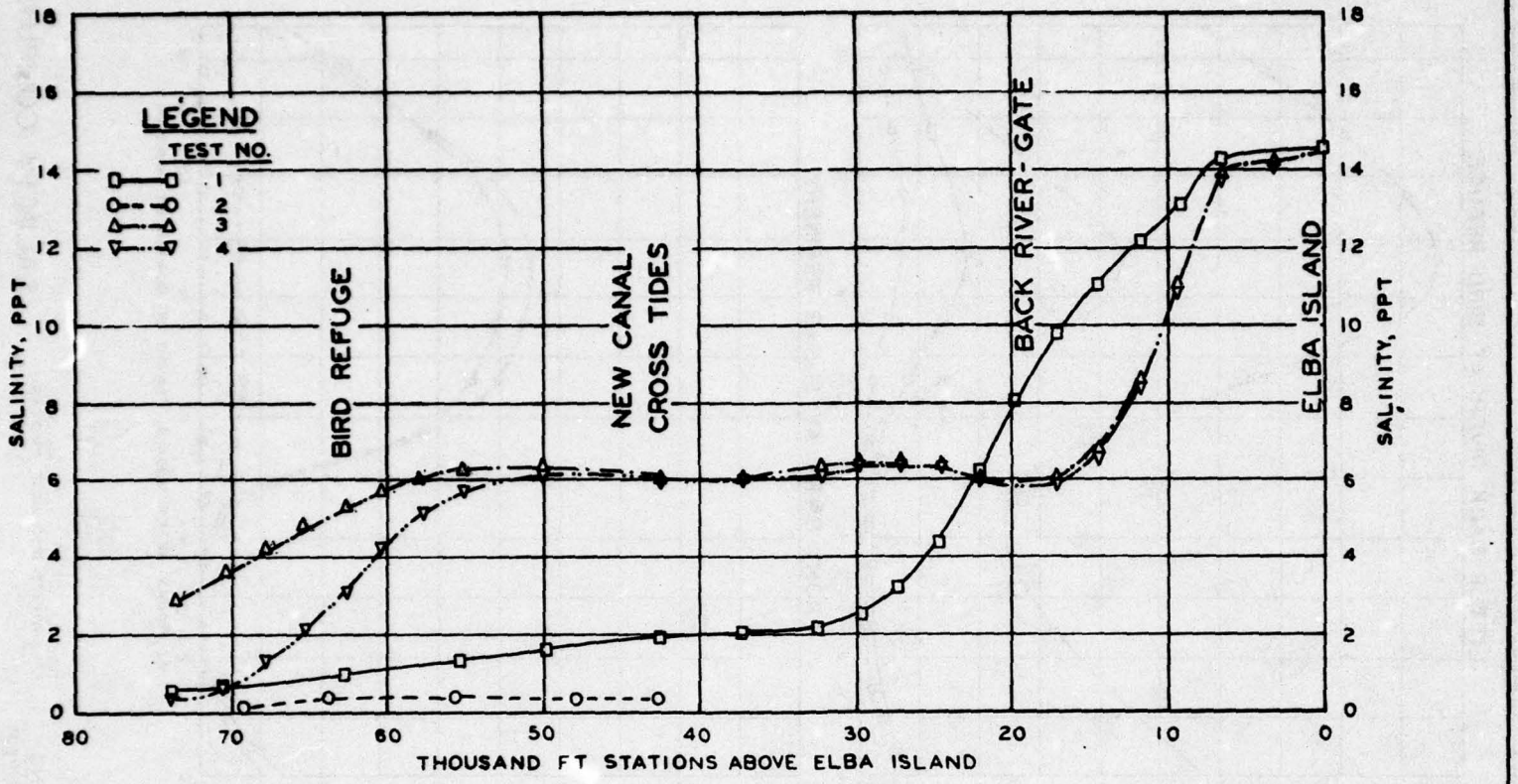

HIGH-WATER SLACK
SALINITY PROFILES
BACK RIVER

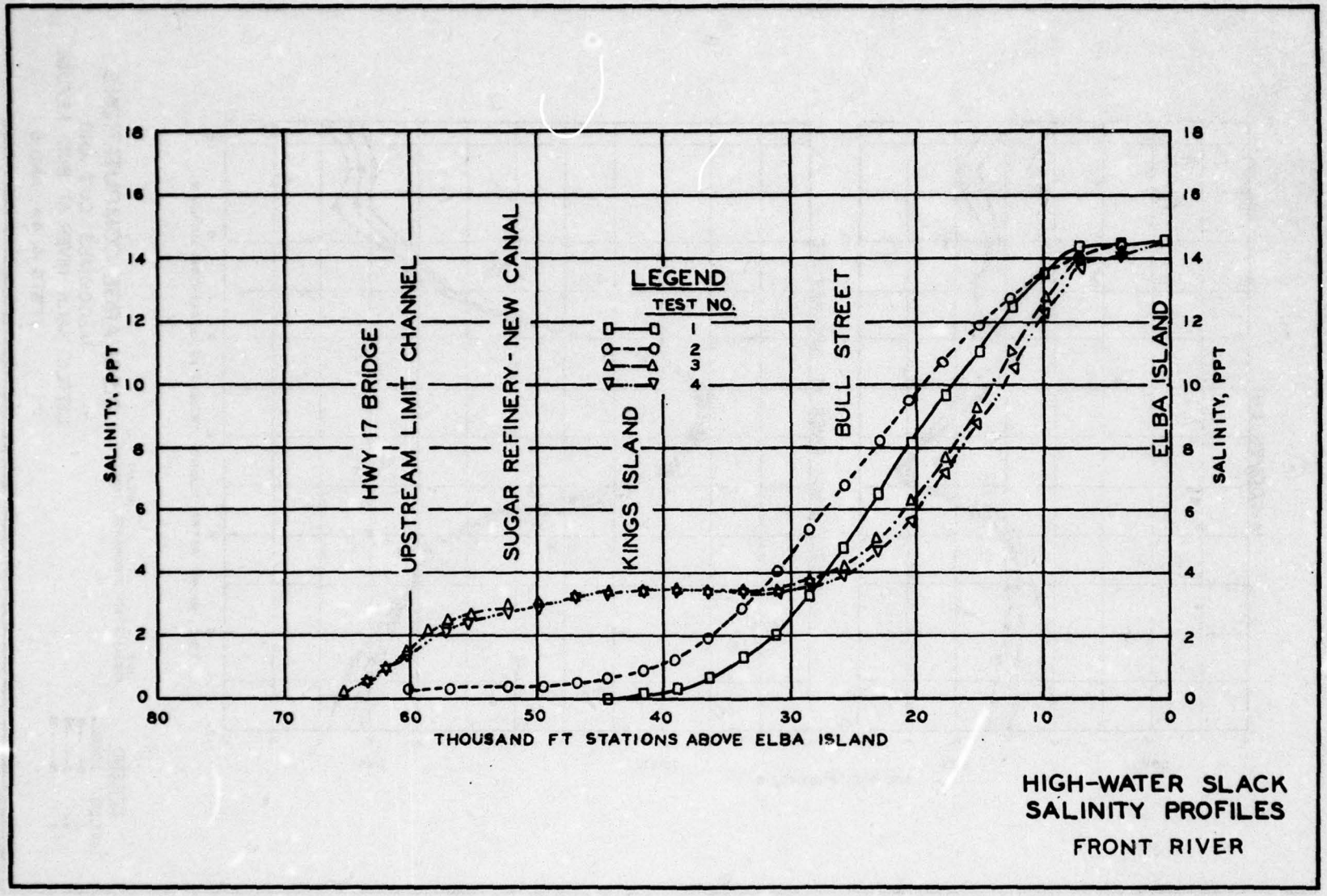

HIGH-WATER SLACK
SALINITY PROFILES
FRONT RIVER

PLATE 15

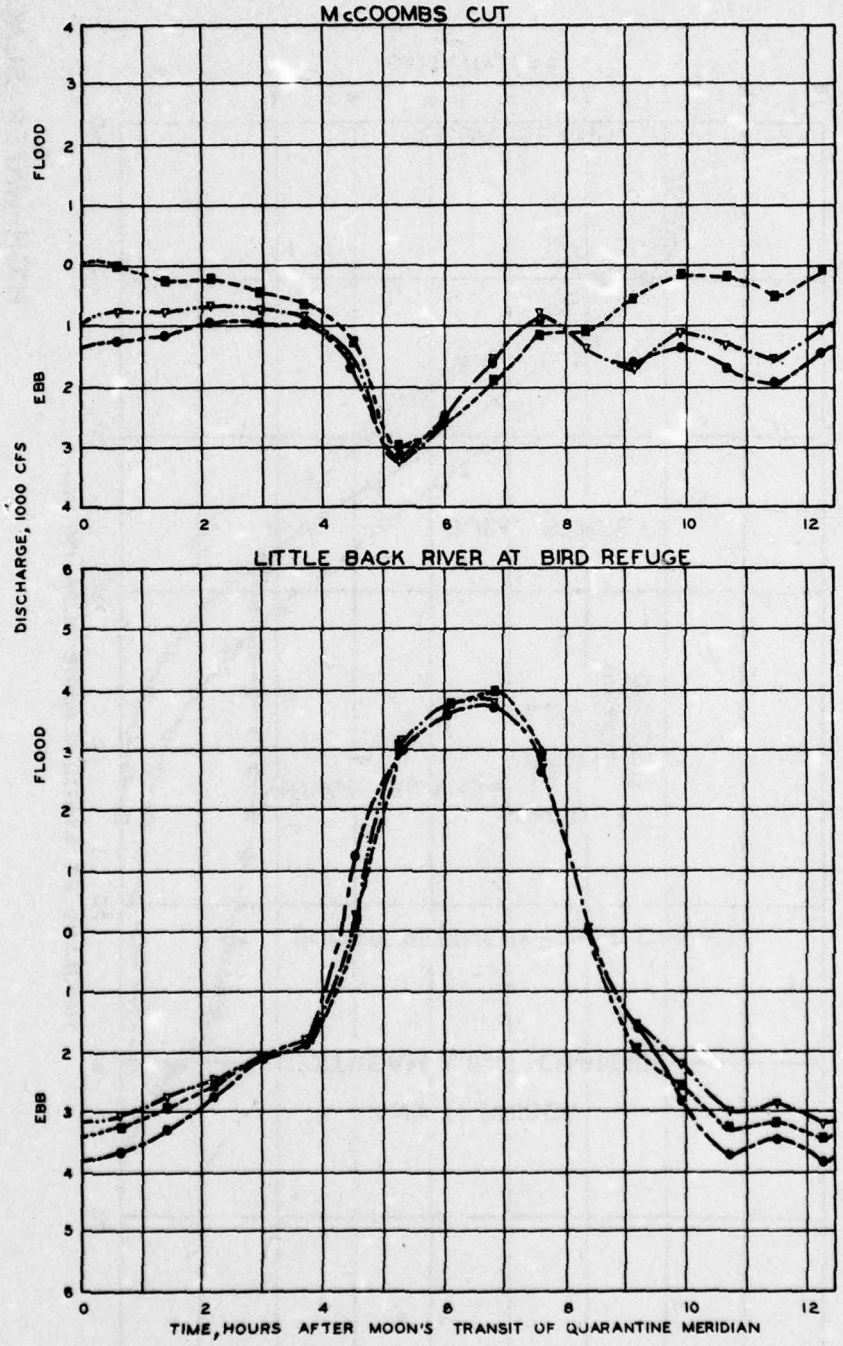

LEGEND

TEST NO.	SYMBOL
4	
4A	
5	

TIDE.....MEAN
FRESHWATER DISCHARGE..7300 CFS

DISCHARGE COMPUTATIONS
McCOOMBS CUT AND
LITTLE BACK RIVER AT BIRD REFUGE
TESTS 4, 4A, AND 5

PLATE 16

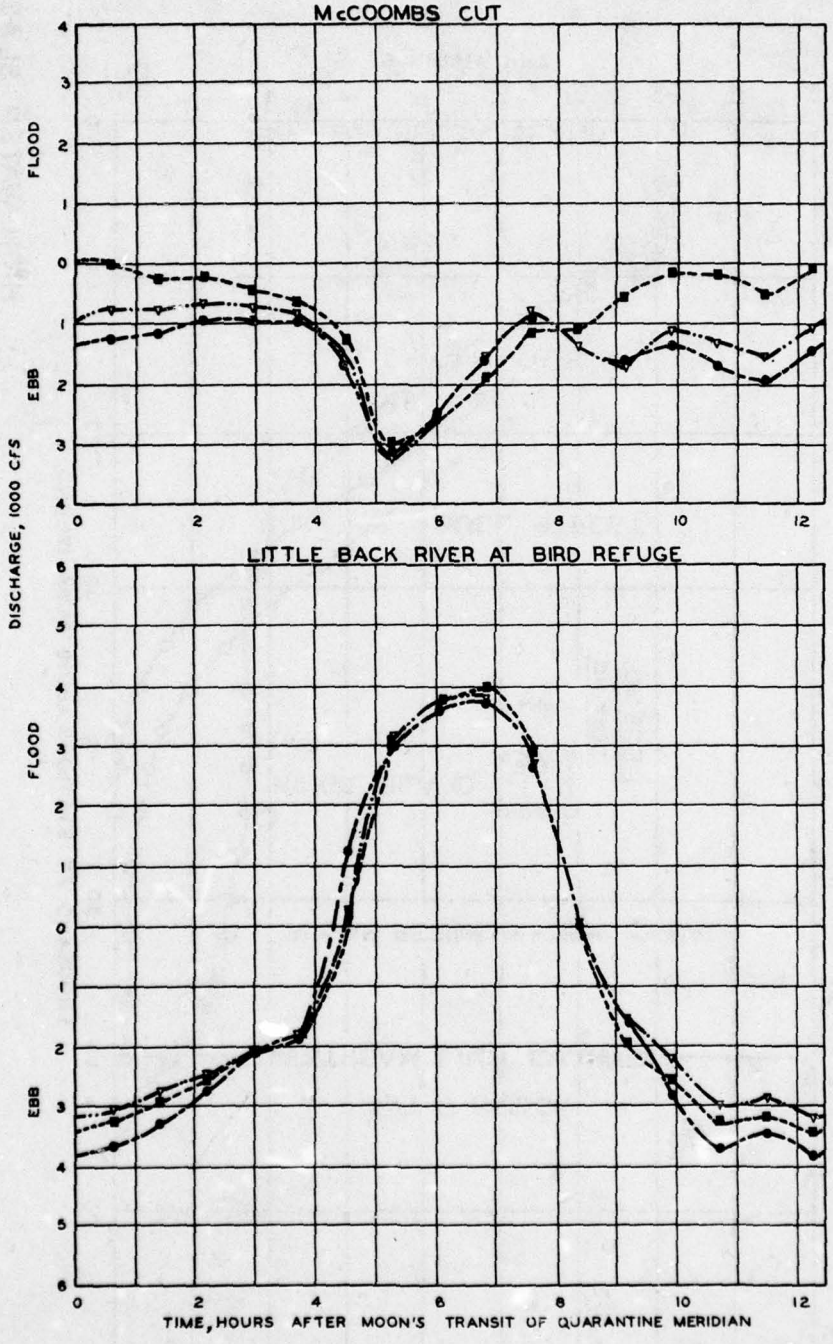

LEGEND

TEST NO.	SYMBOL
4	
4A	
5	

TIDE.....MEAN
FRESHWATER DISCHARGE..7300 CFS

DISCHARGE COMPUTATIONS
McCOOMBS CUT AND
LITTLE BACK RIVER AT BIRD REFUGE
TESTS 4, 4A, AND 5

PLATE 16

APPENDIX A: THE HYDRODYNAMIC MODEL

Introduction

1. The numerical study of the upper reaches of the Savannah Estuary was based on an application of the one-dimensional long-wave equations. The computer code which was developed is also applicable to the solution of other problems where the situation is topologically similar and where long-period tidal flows or natural floods are of interest. The program is not suited to investigations in which the movement of bores must be considered.

2. Topologically, the upper reaches of the Savannah Estuary consist of a network of interconnected channels and the computer program developed to support this investigation was written to allow the determination of tidal motion for entirely arbitrary channel networks. As a matter of definition, we shall refer to a reach of channel between two junctions as a branch and to the junctions as nodes; the extremity of a channel, not at a node, is referred to as a boundary. The treatment that was applied to the determination of flow conditions at a junction is quite general and the code, therefore, was written to permit the connection of two or more branches at a junction or a node. The junction algorithm is also applicable to the determination of tidal flows at places where there is a sudden change in channel geometry and nodes, therefore, were put at locations where sudden changes in channel geometry occurred.

3. Several methods of deriving the one-dimensional long-wave equations are available. The control volume approach was particularly useful in making decisions pertinent to the design of the numerical model. The key result of this reasoning being that the long-wave approximate momentum equation is not applicable, i.e., not descriptive of the phenomenon, at the junction of channels or at locations where there are sudden changes in channel configuration. This is the case because in these instances, there are forces that influence the flow but that are not accounted for in the approximation. This conclusion

is, of course, not original (see Lamb).*

Numerical Hydraulics for Channel Networks

4. The one-dimensional long-wave equations used in this study were

$$\frac{\partial Q}{\partial t} = -\frac{\partial}{\partial x} uQ - gA \frac{\partial \eta}{\partial x} - \frac{gQ|Q|}{AC^2R} \tag{A1}$$

and

$$\frac{\partial A}{\partial t} = -\frac{\partial Q}{\partial x} \tag{A2}$$

where

Q = discharge

u = mean velocity, i.e., the velocity averaged over the cross section

A = cross-sectional area

η = water-surface elevation

C = Chezy coefficient

R = hydraulic radius

g = gravitational acceleration constant

x = longitudinal distance along the channel

t = time

In the computation C was

$$C = \frac{1.49}{n} R^{1/6} \tag{A3}$$

---

* For the case of inviscid tidal motion in a channel of constant width with a smooth bottom, the forces accounted for by the momentum equation are the pressure forces acting at the two ends of the control section and the pressure force acting along the bottom of the channel. If there is a step in the channel, an additional force not included in the above acts on any control reach lying across the sudden rise. Lamb treats this problem which is that of wave reflection and transmission. (Sir Horace Lamb. 1932. Hydrodynamics, 6 ed., Dover Publications.)

where n is Manning's roughness coefficient.

5. The numerical approximation of the one-dimensional long-wave equations, which was used in this analysis, may be derived in several ways. The one that follows elucidates the conservative characteristics of the approximations. Suppose that a branch of the channel network is divided into an even number of equal segments, $2n$. There are then (including both ends) $2n + 1$ stations along the channel. We suppose these to be located at x_1, x_2, x_3, ... , x_{2n+1}. For convenience we set

$$Q_i = Q(x_i,t) , \quad \dot{Q}_i = \frac{\partial}{\partial t} Q(x_i, t)$$
$$A_i = A(x_i,t) , \quad \dot{A}_i = \frac{\partial}{\partial t} A(x_i, t) \tag{A4}$$

Integrating Equation A2 and applying Leibnitz's rule results in

$$\frac{d}{dt} \int_{x_{i-1}}^{x_{i+1}} A \, dx = Q_{i-1} - Q_{i+1} ; \quad i = 2, 3, \ldots , 2n - 1 \tag{A5}$$

If the integral on the left of Equation A5 is approximated by the midpoint rule, the result is

$$\dot{A}_i = \frac{1}{2\delta x} (Q_{i-1} - Q_{i+1}) ; \quad i = 2, 3, \ldots , 2n - 1 \tag{A6}$$

where δx is the uniform length of the segments.* Similarly, Equation A1 becomes

---

* The use of the midpoint rule is arbitrary in the sense that Simpson's rule could also be used, or if a different choice of elements were made any other numerical quadrature formula. Should Simpson's rule have been used, the result would have been

$$\frac{1}{6} \dot{A}_{i-1} + \frac{2}{3} \dot{A}_i + \frac{1}{6} \dot{A}_{i+1} = \frac{1}{\delta x} (Q_{i+1} - Q_{i-1})$$

which is two orders of magnitude more accurate than Equation A4. More computations would, however, be required.

$$\dot{Q}_i = \frac{1}{2\delta x}\left[(uQ)_{i-1} - (uQ)_{i+1}\right] + \frac{gA_i}{2\delta x}(\eta_{i-1} - \eta_{i+1}) - \left(g\frac{Q|Q|}{AC^2R}\right)_i \quad ; \qquad (A7)$$

$$i = 2, 3, \ldots, 2n - 1$$

when the approximation

$$\int_{x_{i-1}}^{x_{i+1}} F\dot{G}\, dx = \int_{x_{i-1}}^{x_{i+1}} F_i\dot{G}\, dx + O(\delta x^3) \qquad (A8)$$

has been applied. The analytical procedure just applied has reduced the problem of solving a pair of partial differential equations to that of solving a system of ordinary differential equations whose solution approximates that of the original problem. The procedure has numerous applications and is referred to as Kantorovich's method or the method of undetermined functions.

6. The set of double intervals, x_{i-1} to x_{i+1}, covers the branch in the sense that there is no open set along the branch not lying in an interval and that every connected open set along the branch which does not contain an x_i lies in a unique interval. Also, Equation A6 clearly implies that the rate of mass flux out of the double interval x_{i-2}, x_i is equal to the rate of mass flux into the double interval x_i, x_{i+2}. Hence, it follows that mass is conserved, i.e., none is lost or gained by the approximation given in Equation A6.

7. Momentum, however, is conserved only up to an order of δx^3 because of the approximation indicated by Equation A8. It would be feasible to use a more accurate approximation than Equation A8, but this would have been pointless because the midpoint rule used in deriving Equations A6 and A7 is only accurate to the order δx^3.

Numerical Integration

8. The $2n - 1$ first order ordinary differential equations of

Equation A6 and the $2n - 1$ first order ordinary differential equations of Equation A7 must be solved. This could be accomplished with any of a number of the various numerical methods for solving systems of first-order ordinary differential equations. The two-point predictor-corrector method was used in this study. To explain the method we first note that Equations A6 and A7 could be written as a system of $4n - 2$ ordinary differential equations

$$\dot{\underset{\sim}{z}} = \underset{\sim}{f}\,(t, \underset{\sim}{z}) \tag{A9}$$

where $\underset{\sim}{z}$, $\underset{\sim}{f}$, and $\dot{\underset{\sim}{z}}$ denote the vectors

$$\begin{aligned} \underset{\sim}{z} &= (z_1, z_2, \ldots, z_{4n-1}) \\ \underset{\sim}{f} &= (f_1, f_2, \ldots, f_{4n-1}) \\ \dot{\underset{\sim}{z}} &= (\dot{z}_1, \dot{z}_2, \ldots, \dot{z}_{4n-1}) \end{aligned} \tag{A10}$$

The predictor algorithm is

$$\underset{\sim}{z}^*_{j+1} = \underset{\sim}{z}_j + \underset{\sim}{f}_j\, \delta t \tag{A11}$$

where

$$\underset{\sim}{z}_j = \underset{\sim}{z}(t_j)\,, \quad \underset{\sim}{f}_j = \underset{\sim}{f}(t_j, \underset{\sim}{z}_j) \tag{A12}$$

and

$$\delta t = t_{j+1} - t_j \tag{A13}$$

The corrector algorithm is

$$\underset{\sim}{z}_{j+1} = \underset{\sim}{z}_j + \frac{1}{2}\,(\underset{\sim}{f}_j + \underset{\sim}{f}^*_{j+1})\, \delta t \tag{A14}$$

where

$$\underset{\sim}{f}^*_{j+1} = \underset{\sim}{f}(t_{j+1}, z^*_{j+1})$$

To apply these algorithms $\underset{\sim}{z}$ must be known at the time t_j. The quantity $\underset{\sim}{z}^*_{j+1}$ is the prediction of $\underset{\sim}{z}$ for the time t_{j+1}. After it is computed, an improved or corrected estimate of $\underset{\sim}{z}$ at time t_{j+1} is made by applying Equation A14.

9. The predictor-corrector method was employed because it was known that the method is well suited to the integration of ordinary differential equations describing oscillations. No comparison of the computational efficiency of this algorithm with others available was made. Our current inclination for future studies would be to make a more thorough investigation of this with the view of using the predictor-corrector scheme for an initial time-step and the central difference scheme

$$\underset{\sim}{z}_{j+1} = \underset{\sim}{z}_{j-1} + 2\underset{\sim}{f}_j \delta t$$

thereinafter.

The Junction of Channels

10. In preceding sections, a numerical method was given for estimating the quantities Q and A at time $t + \delta t$ given the values of these quantities at time t. The numerical formulas do not, however, apply to either the first or last station along a branch. Computation of Q and A at the ends of a branch is considered in this section.

11. Q and A may be assumed to be known at all stations at time t and using numerical algorithms indicated in preceding sections Q and A may be computed at times $t + \delta t$ at all interior stations. Hence, at a typical node β as depicted in Figure A1, the discharges and cross-sectional areas are known as stations $(a,1)$, $(b,2)$, and $(c,2)$ which are interior stations.

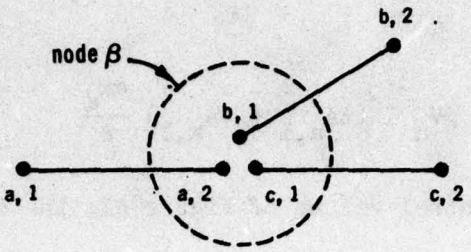

Figure A1

Our notation is that the first variable, i.e., a , b , or c , denotes the branch and the second variable denotes the station. It is assumed that there is no storage at the node; and conservation of mass, therefore, requires that

$$Q_{a,2} - Q_{b,1} - Q_{c,1} = 0 \tag{A15}$$

It was also assumed that

$$\eta_{a,2} = \eta_{b,1} = \eta_{c,1} \tag{A16}$$

which is an assumption that there was no significant head loss at the junctions.

12. These compatibility conditions are used along with the integral form of the continuity equation in finite difference form

$$\frac{\delta \Psi}{\delta t} = \Sigma \bar{Q}_i - \Sigma \bar{Q}_o \tag{A17}$$

where

$$\bar{Q} \simeq \frac{1}{2} (Q_t + Q_{t+\delta t}) \tag{A18}$$

that is, the rate of change in volume is equal to the difference in discharges through the node. The trapezoidal rule, which is accurate to third order, was used for volume computations.

$$\Psi_a \simeq (A_{a,1} + A_{a,2}) \frac{\delta x_a}{2} \tag{A19}$$

or

$$\delta\Psi_a \simeq (\delta A_{a,1} + \delta A_{a,2}) \frac{\delta x_a}{2} \tag{A20}$$

For the "Y" shaped control volume of Figure A1, the continuity equation is then written as

$$(\delta A_{a,1} + \delta A_{a,2}) \frac{\delta x_a}{2} + (\delta A_{b,1} + \delta A_{b,2}) \frac{\delta x_b}{2} + (\delta A_{c,1} + \delta A_{c,2}) \frac{\delta x_c}{2} = (\bar{Q}_{a,1} - \bar{Q}_{b,2} - \bar{Q}_{c,2}) \delta t \tag{A21}$$

The values of

$$\delta A_{a,1} \frac{\delta x_a}{2}, \quad \delta A_{b,2} \frac{\delta x_b}{2}, \quad \delta A_{c,2} \frac{\delta x_c}{2}$$

are known at time level $t + \delta t$ and it is convenient to define the quantity S_Ψ by

$$S_\Psi = \delta A_{a,1} \frac{\delta x_a}{2} + \delta A_{b,2} \frac{\delta x_b}{2} + \delta A_{c,2} \frac{\delta x_c}{2} \tag{A22}$$

Similarly, the discharge values appearing in Equation A21 are known at time level $t + \delta t$ and we define

$$S_Q = (\bar{Q}_{a,1} - \bar{Q}_{b,2} - \bar{Q}_{c,2}) \delta t \tag{A23}$$

Thus, Equation A21 reduces to

$$\delta A_{a,2} \frac{\delta x_a}{2} + \delta A_{b,1} \frac{\delta x_b}{2} + \delta A_{c,1} \frac{\delta x_c}{2} = S_Q - S_\Psi \tag{A24}$$

Because of Equation A16 we may define a function F_β for each node as a function of water-surface elevation η,

$$F_\beta(\eta) = A_{a,2} \frac{\delta x_a}{2} + A_{b,1} \frac{\delta x_b}{2} + A_{c,1} \frac{\delta x_c}{2} \tag{A25}$$

The functions F_β are known functions, i.e., data describing the variation of cross-sectional area with depth are data input into the computation. Introduction of this definition reduces Equation A24 to

$$\delta F_\beta(\eta) = S_Q - S_\Psi \tag{A26}$$

where

$$F_\beta[\eta(t + \delta t)] = F_\beta[\eta(t)] + \delta F_\beta(\eta) \tag{A27}$$

Thus, the node problem is seen to be reduced to that of finding that value of η for which a prescribed function F_β assumes a previously computed numerical value $S_Q - S_\Psi$. This problem was solved by inverse interpolation between known values of F_β.

13. Once $\eta_\beta(t+\delta t)$, i.e. η at the node β at time $t + \delta t$, is computed the cross-sectional areas of the stations at the node, i.e., $A_{a,2}$, $A_{b,1}$, and $A_{c,1}$ may be computed, and then finally $Q_{a,2}$, $Q_{b,1}$, and $Q_{c,1}$ may be computed from the approximate continuity relations

$$\overline{Q}_{a,2} = -\frac{\delta x_a}{2\delta t}(\delta A_{a,1} + \delta A_{a,2}) + \overline{Q}_{a,1} \tag{A28}$$

$$Q_{a,2}(t + \delta t) = 2\overline{Q}_{a,2} - Q_{a,2}(t) \text{ , etc.} \tag{A29}$$

14. It is important to note that the mass conservation compatibility condition expressed by Equation A15 is satisfied by the Q's computed from Equation A29. An interesting property of the computer program used in solving the channel network problem is that any of the usual errors in data preparation which we have made in the Savannah study have produced numerical outputs in which Equation A15 was not satisfied and this compatibility condition has been a good error check.

Network Identification

15. Equations A16-A27 were given for a specific example, i.e., the

typical junction indicated in Figure A1. In application, a more general procedure has been adopted. A minimal explanation of the convention used in network identification is needed to facilitate a description of this.

16. Every station was given a unique station identification such that along each branch the station ID's formed a consecutive sequence of integers. Branches were also assigned unique integer ID's and a table of the first and last stations of a branch versus branch ID constructed. The convention that the positive sense of a branch was in the direction of increasing station ID was adopted. This convention fixes for each branch the direction of positive flow and positive slope. Finally, a table of branch ID's versus node ID was constructed and was used with the convention that if positive displacement along a branch implied movement toward the relevant node the flux into the node from the branch was positive. The sign of the flux for the various branches was also tabulated as a function of node ID .

17. Let the sign of the node flux for a branch α at node β be*

$$\sigma_{\alpha\beta} = \begin{cases} +1 \text{ if the largest station number for branch } \alpha \text{ is at node } \beta \\ -1 \text{ if the lowest station number for branch } \alpha \text{ is at node } \beta \end{cases} \tag{A30}$$

and let K be the set of ID's of all branches ending at a node. Two other sets of ID's are easily determined. These are**

$$M = \left\{ m_{\alpha\beta} \middle| m_{\alpha\beta} = \text{the maximum station ID for branch ending at node } \beta \text{ if } \sigma_{\alpha\beta} = 1 \text{ ; or } m_{\alpha\beta} = \text{the minimum station ID if } \sigma_{\alpha\beta} = -1 \right\} \tag{A31}$$

---

* The $\sigma_{\alpha\beta}$ table must be constructed prior to the execution of the computer program and is input (control) data.

** The long | is known as the universal or set qualifier and may be read as "such that," the {} may be read as the set of all elements.

$$N = \left\{ n_{\alpha\beta} \mid n_{\alpha\beta} = m_{\alpha\beta} - \sigma_{\alpha\beta} \right\} \tag{A32}$$

Using Equations A30, A31, and A32, the generalizations of Equations A22 and A23 are

$$S_{\Psi} = \sum_{n \epsilon N} \delta A_n \frac{\delta x}{2} \alpha \tag{A33}$$

$$S_Q = \sum_{n \epsilon N} Q_n \sigma_{\alpha\beta} \tag{A34}$$

where $n \epsilon N$ is to be read as n is an element of the set N. Equation A25 is generalized as

$$F_\beta(\eta) = \sum_{m \epsilon M} \delta A_m \frac{\delta x}{2} \alpha \tag{A35}$$

Equation A26 is unchanged, i.e.,

$$\delta F_\beta = S_Q - S_{\Psi} \tag{A36}$$

As previously explained, the equation is used to determine η and thence the A's for the stations at the nodes. The generalization of Equation A28 becomes

$$\overline{Q}_n = \overline{Q}_m - \frac{\delta x_\alpha}{2\delta t} (\delta A_m + \delta A_n) \sigma_{\alpha\beta} \tag{A37}$$

Equation A29 is unchanged, i.e.,

$$Q_n (t + \delta t) = 2\overline{Q}_n - Q_n(t) \tag{A38}$$

18. We close this section by noting that the essential ideas are presented by the example of the previous section. The equations presented here are given as a matter of record.

Boundary Conditions

19. Various approaches to the treatment of boundary conditions

were tried, but ultimately the control volume approach used for the junction problem was adopted. Assume that branch α has an extremity at station m not located at a node. We define σ by

$$\sigma_\alpha = \begin{cases} 1 \text{ if } m \text{ is the largest ID for the branch} \\ -1 \text{ if } m \text{ is the lowest ID for the branch} \end{cases} \tag{A39}$$

and n by

$$n = m - \sigma_\alpha \tag{A40}$$

Using the approximation of Equation A20 and Equation A17

$$(\delta A_m + \delta A_n) \frac{\delta x_\alpha}{2} = \sigma_\alpha (\bar{Q}_n - \bar{Q}_m) \tag{A41}$$

Station m is at the boundary and either η or Q must be prescribed there as a boundary condition. Also, station n is an interior station and A_n and $\bar{Q}_n$ may be assumed to be already computed; and since A is a prescribed function of η at every station, either Q_m or A_m is also known. The remaining unknown is either

$$\delta A_m = \sigma_\alpha (Q_n - Q_m) \frac{2}{\delta x_\alpha} - \delta A_n \tag{A42}$$

or

$$\bar{Q}_m = \bar{Q}_n - \sigma_\alpha (\delta A_m + \delta A_n) \frac{\delta x_\alpha}{2} \tag{A43}$$

where $Q_m(t + \delta t)$ may be computed by Equation A29.

APPENDIX B: THE SALINITY MODEL

Introduction

1. Numerous problems beset the predictive determination of the salinity distribution in a real channel network. In particular, the flow is turbulent and it is completely infeasible to compute with a time increment δt and space increments, δx , δy , δz , which would permit the solution of the equations that describe the process exactly. As a result, simplifying assumptions and correspondent empirical approximations must be introduced.

2. Techniques for accomplishing the necessary simplification and empiricism have been the subject of numerous research efforts. A brief review of the mechanics of turbulent diffusion and of dispersive processes is given in the next section. It is hoped that this discussion will provide some insight into the process and the related limitations of the resultant mathematical model.

3. The one-dimensional convective dispersion equation is usually used to describe dispersive processes in channels, and it has been found that for a proper spatially dependent choice of the dispersion coefficient E a good empirical fit to observed salinity distributions for various estuarine systems may be obtained. Unfortunately, attempts to correlate the dispersion coefficient with channel and flow characteristics have not been entirely successful, in that there is very little coherence between estimated dispersion coefficients and proposed empirical formulas. Known finite-difference formulas of convective processes suffer from the phenomenon of numerical dispersion. Let E_n be the numerical dispersion coefficient, E_a the actual dispersion coefficient which exists at least as a matter of formal definition, and E_e be the dispersion coefficient arrived at by empirical data analysis or mathematical model calibration. Clearly,

$$E_e = E_a - E_n$$

Also, E_n is dependent on the numerical model, the discretization parameters δx and δt used, and the convective rate u. It is concluded that the existence of and variations in E_n may at least in part explain variations in E_e. An example related to the problem of numerical flood routing showed that E_a and E_n are practically equal.

4. The great empirical variability in observed disperion coefficients raises questions about the utility of numerical predictions of dispersion processes. Certainly, results must be interpreted in terms of the specific problem being investigated and qualified as to the nature of the solution provided. In this context, three logical questions are significant:

a. How sensitive is the numerical solution to variations in the dispersion coefficient?

b. Do numerical solutions indicate the same relative result independent of the dispersion coefficient?

c. Is the numerical solution(s) consistent with the behavior of other (hydraulic) flow characteristics or changes?

The extent to which these questions may be affirmatively answered is indicative of the reliability that may be associated with the numerical solution.

Turbulent Diffusion and Dispersion in Channels

5. In this section, an idealized channel in which there is no lateral velocity is assumed. Let x be the horizontal coordinate and y be the vertical coordinate and u and v be the velocities in these respective directions. Also, let s be the concentration of a solute which is conserved. The governing equation may be shown to be

$$\frac{\partial s}{\partial t} + \frac{\partial us}{\partial x} + \frac{\partial vs}{\partial y} = 0 \tag{B1}$$

We assume that we may decompose s, u, and v into component

$$\begin{aligned} s &= \bar{s} + s' \\ u &= \bar{u} + u' \\ v &= \bar{v} + v' \end{aligned} \tag{B2}$$

such that the primed part is that which is due to turbulent fluctuations. In the manner devised by Osborne Reynolds (see Schlichting*) Equation B1 may then be transformed into

$$\frac{\partial \bar{s}}{\partial t} + \frac{\partial \bar{u}\bar{s}}{\partial x} + \frac{\partial \bar{v}\bar{s}}{\partial y} = - \frac{\partial \overline{u's'}}{\partial x} - \frac{\partial \overline{v's'}}{\partial y} \tag{B3}$$

For practical computation, the terms on the right of Equation B3 must be empirically approximated. We assume

$$\begin{pmatrix} \overline{u's'} \\ \\ \overline{v's'} \end{pmatrix} = - \begin{pmatrix} D_{1,1} & D_{1,2} \\ \\ D_{2,1} & D_{2,2} \end{pmatrix} \begin{pmatrix} \frac{\partial \bar{s}}{\partial x} \\ \\ \frac{\partial \bar{s}}{\partial y} \end{pmatrix} \tag{B4}$$

and the diffusion matrix D is not in any way dependent on $\bar{s}(x,y,t)$. Equation B4 is more general than the relations which are usually assumed, but may be shown to be less general than the actual process, i.e., Equation B4 is at best an approximation.

6. It will, however, suffice in our investigation of the main features of the mechanics of the diffusion process for tidal motion in a channel. Let us now nondimensionalize Equations B3 and B4 by setting

$$x = x^*L \ , \quad y = y^*h \ , \quad u = u^*\sqrt{gh} \ , \quad v = v^*\sqrt{gh} \ , \quad t = t^*L/\sqrt{gh} \ , \tag{B5}$$

$$D_{i,j} = D^*_{i,j} \, \sigma \sqrt{gh}$$

where L is a reference length and h is a reference vertical dimension and the scaling parameter σ is for now left undefined. Combining Equations B3 and B4 results in

$$\frac{\partial s}{\partial t} + \frac{\partial us}{\partial x} + \frac{\partial vs}{\partial y} = \frac{\partial}{\partial x} \left(D_{1,1} \frac{\partial s}{\partial x} + D_{1,2} \frac{\partial s}{\partial y} \right) + \frac{\partial}{\partial y} \left(D_{2,1} \frac{\partial s}{\partial x} + D_{2,2} \frac{\partial s}{\partial y} \right) \tag{B6}$$

where the "—" has now been dropped.

---

* Dr. Hermann Schlichting. 1955. Boundary Layer Theory, Pergamon Press.

7. Nondimensionalizing Equation B6 with respect to the transform given in Equation B5 results in

$$\frac{\sqrt{gh}}{L}\frac{\partial s}{\partial t^*} + \frac{\sqrt{gh}}{L}\frac{\partial u^* s}{\partial x^*} + \frac{\sqrt{gh}}{h}\frac{\partial v^* s}{\partial y^*} = \frac{1}{L}\frac{\partial}{\partial x^*}\left(\sigma\sqrt{gh}\, D^*_{1,1}\frac{1}{L}\frac{\partial s}{\partial x^*} + \sigma\sqrt{gh}\, D^*_{1,2}\frac{1}{h}\frac{\partial s}{\partial y^*}\right) + \frac{1}{h}\frac{\partial}{\partial y^*}\left(\sigma\sqrt{gh}\, D^*_{2,1}\frac{1}{L}\frac{\partial s}{\partial x^*} + \sigma\sqrt{gh}\, D_{2,2}\frac{1}{h}\frac{\partial s}{\partial y^*}\right) \tag{B7}$$

or

$$\varepsilon\left(\frac{\partial s}{\partial t^*} + \frac{\partial u^* s}{\partial x^*}\right) + \frac{\partial v^* s}{\partial y^*} = \frac{\sigma h}{L^2}\frac{\partial}{\partial x^*} D^*_{1,1}\frac{\partial s}{\partial x^*} + \frac{\sigma}{L}\frac{\partial}{\partial x^*} D^*_{1,2}\frac{\partial s}{\partial y^*} + \frac{\sigma}{L}\frac{\partial}{\partial y^*} D^*_{2,1}\frac{\partial s}{\partial x^*} + \frac{\sigma}{h}\frac{\partial}{\partial y^*} D^*_{2,2}\frac{\partial s}{\partial y^*} \tag{B8}$$

where $\varepsilon = h/L$

7. For tidal flows the parameter ε may be assumed to be the depth of the channel divided by the tidal wavelength and thus ε is a very small number. Also, $\partial s/\partial t^*$, $\partial s/\partial x^*$, and $\partial s/\partial y^*$ should be the same order of magnitude, and it may be shown that $D_{1,1}$, $D_{1,2}$, $D_{2,1}$ and $D_{2,2}$ or their nondimensional counterparts are of the same order. An examination of Equation B8 then leads us to conclude that

a. $\partial v^* s/\partial y$ is of order ε times the quantity in parentheses on the left of Equation B8.

b. Turbulent diffusion is of considerable importance in the dispersion process and the solution of Equation B8 cannot be in reasonable correspondence to the physical phenomena, unless the largest turbulent diffusion term(s) are of the same order of magnitude as the dominant convective terms(s).

The largest diffusion term is

$$\frac{\sigma}{h}\frac{\partial}{\partial y^*} D^*_{2,2}\frac{\partial s}{\partial y^*}$$

and observation b, therefore, implies that

$$\frac{\sigma}{h} = \varepsilon \tag{B9}$$

or

$$\sigma = \frac{h^2}{L} \tag{B10}$$

The resulting first order model, therefore, is

$$\frac{\partial s}{\partial t} + \frac{\partial us}{\partial x} = \frac{\partial}{\partial y} D_{2,2} \frac{\partial s}{\partial y} \tag{B11}$$

8. Pritchard* has made an extensive analysis of field data obtained from the James River estuary. His analysis was of data averaged over a tidal cycle. His results indicate that vertical diffusion was much greater than horizontal diffusion and that horizontal convection was much greater than vertical convection as this analysis indicates they should be. Li** presents an analysis of a number of not basically dissimilar problems of quasi-parallel turbulent flow and reaches the same conclusion.

9. To obtain a better feel for the implications of Equation B11, let us first assume that $D_{2,2}$ equals zero. In this case,

$$\frac{\partial s}{\partial t} + \frac{\partial us}{\partial x} = 0$$

and the behavior of s is as shown in Figure B1. In particular, for a simple shear flow, i.e. u dependent only on y, the solution may be entirely characterized by noting that along the curve

$$x(y, t_o + \tau) = u(y)\ (t_o + \tau)$$

s as a function of y is exactly the same as the distribution of s as function of y along the curve $x = 0$ at time t_o.

---

* D. W. Pritchard. 1958. "The Equation of Mass Continuity and Salt Continuity in Estuaries," Journal of Marine Research, Vol 17, pp 412-423.

** Li, Wen-Hsuing. 1972. "Effects of Dispersion on DO Sag in Uniform Flow," Proceedings, American Society of Civil Engineers, Vol 98, No. SA1.

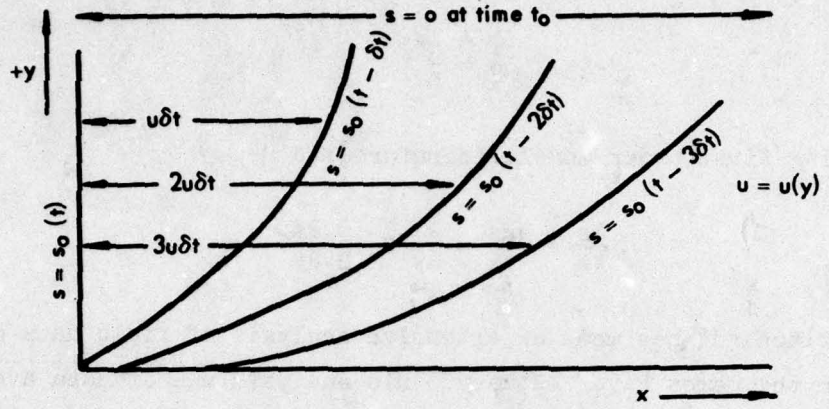

Figure B1. Graphical solution of $\partial s/\partial t + u\ \partial s/\partial x = 0$. For a simple shear flow

10. Secondly, let us suppose that $u = 0$ and that $D_{2,2}$ is independent of y . Equation B11 reduces to

$$\frac{\partial s}{\partial t} = D_{2,2} \frac{\partial^2 s}{\partial y^2}$$

and since there can be no flux of the solute across the bottom of the channel, $y = 0$, or through the free surface $y = h$

$$\frac{\partial s}{\partial y}\Big|_{y=0} = \frac{\partial s}{\partial y}\Big|_{y=h} = 0$$

A solution of this problem is

$$s = s_A + \sum_{j=1}^{\infty} e^{-D\lambda_j^2 t} \cos \lambda_j y$$

where

$$\lambda_j = j \frac{\pi}{h}$$

Evidently then the effect of vertical diffusion is to smooth out whatever variation of s occurs in the vertical direction. Horizontal

convection has the countering effect of converting longitudinal gradients in s into vertical gradients.

11. Finally, let us take up the problem of obtaining a one-dimensional model. Integrating Equation B11 with respect to y results in

$$\frac{\partial \tilde{s}}{\partial t} + \frac{\partial}{\partial x}\frac{1}{h}\int_o^h usdy = \frac{D_{2,2}}{h}\frac{\partial s}{\partial y}\bigg|_{y=h} - \frac{D_{2,2}}{h}\frac{\partial s}{\partial y}\bigg|_{y=0} \qquad \text{(B12)}$$

where the superscript ~ denotes an average over the depth. The no-flux condition at the free surface and bottom of the channel reduces the right-hand side of Equation B12 to zero, or

$$\frac{\partial \tilde{s}}{\partial t} + \frac{\partial}{\partial x}\frac{1}{h}\int_o^h usdy = 0 \qquad \text{(B13)}$$

As a matter of formal definition, Equation B13 may be written as (as it has been in practical applications)

$$\frac{\partial \tilde{s}}{\partial t} + u\frac{\partial \tilde{s}}{\partial x} = \frac{\partial}{\partial x} E \frac{\partial \tilde{s}}{\partial x} \qquad \text{(B14)}$$

Equation B14 is disturbing, because there is no analytical technique for obtaining it from Equation B13 and, therefore, no theoretical reason to anticipate that E is a function of some set of variables. Equation B12 is a diffusion equation, whereas Equation B14 is a dispersion equation. It should be noted, however, that the combination of a vertical velocity gradient (i.e., a shear flow) and vertical diffusion cause an apparent horizontal dispersion. Since no theoretical definition of E is possible it may be viewed as an "empirical knob" which when properly twisted will bring the solution of Equation B14 into a best-fit correspondence with a given set or sets of field data. Nothing of course is wrong with this if a proper prescription for twisting the knob can be found and if the approximation is not too sensitive to minor misadjustment.

A Numerical Approximation

12. The one-dimensional model of dispersion for a conservative constituent s, which will now be identified as the saline concentration, is

$$\frac{\partial s}{\partial t} + u \frac{\partial s}{\partial x} = \frac{\partial}{\partial x} E \frac{\partial s}{\partial x} \tag{B15}$$

13. Assuming that E is zero, an approximate solution of Equation B15 is

$$s(x_i, t_{j+1}) = s(x_i - u_{i,j+1}\, \delta t, t_j) \tag{B16}$$

In the numerical computation u and s are known only at the stations along a branch. Let

$$s_{i,j} = s(x_i, t_j) \quad \text{and} \quad u_{i,j} = u(x_i, t_j) \tag{B17}$$

δt was chosen so that

$$u\delta t \leq \delta x \tag{B18}$$

for all branches; and $s_{i,j+1}$ was found by a linear interpolation between $s_{i-1,j}$ and $s_{i,j}$ if $u_{i,j+1}$ was positive or $s_{i,j}$ and $s_{i+1,j}$ if $u_{i,j+1}$ was negative.

14. The algorithm just indicated is subject to numerical dispersion, and it was not found to be essential to add "real" dispersion in order to obtain good agreement between the model and prototype for the Savannah system. In the Savannah study, the model was used to compute steady-state salinity conditions (i.e., repetitive tide and salinity at boundary) rather than transient conditions.

Junctions and Boundaries

15. The one-dimensional dispersion equation was

$$\frac{\partial s}{\partial t} + u \frac{\partial s}{\partial x} = \frac{\partial}{\partial x} E \frac{\partial s}{\partial x} \qquad \text{(B19)}$$

while the mass conservation equation of an incompressible fluid is

$$\frac{\partial A}{\partial t} + \frac{\partial Q}{\partial x} = 0 \qquad \text{(B20)}$$

multiplying Equation B19 by A and Equation B20 by s and adding results in

$$\left(A \frac{\partial s}{\partial t} + s \frac{\partial A}{\partial t}\right) + \left(Q \frac{\partial s}{\partial x} + s \frac{\partial Q}{\partial x}\right) = A \frac{\partial}{\partial x} E \frac{\partial s}{\partial x} \qquad \text{(B21)}$$

or

$$\frac{\partial As}{\partial t} + \frac{\partial Qs}{\partial x} = A \frac{\partial}{\partial x} E \frac{\partial s}{\partial x} \qquad \text{(B22)}$$

If dispersion is ignored (i.e., $E = 0$), Equation B22 reduces to

$$\frac{\partial As}{\partial t} + \frac{\partial Qs}{\partial x} = 0 \qquad \text{(B23)}$$

which is essentially the same as Equation B20.

16. Appropriate compatibility conditions at a node are

$$\sum Qs \text{ (from all branches)} = 0 \qquad \text{(B24)}$$

and

$$s(\text{branch 1 node station}) = s(\text{branch 2-- n node stations}) \qquad \text{(B25)}$$

Recalling that the compatible conditions used in determining the flow at a junction (pages A6-A11) are essentially the same, one sees that the same algorith may be applied.

Let

$$S'_Q = \sum_{n \epsilon N} (sQ)_n \, \sigma_{\alpha\beta} \tag{B26}$$

and

$$S'_\Psi = \sum_{n \epsilon N} \delta(sA)_m \frac{\delta x_\alpha}{2} \tag{B27}$$

One obtains

$$s_\beta \, \delta F_\beta = S'_Q - S'_\Psi \tag{B28}$$

Or, since δF_β is in this case known

$$s_\beta = \frac{S'_Q - S'_\Psi}{\delta F_\beta} \tag{B29}$$

where like S_Q and S_Ψ, S'_Q and S'_Ψ have been previously computed.

17. The same correspondence exists at boundaries, so they will not be discussed separately.

In accordance with letter from DAEN-RDC, DAEN-ASI dated 22 July 1977, Subject: Facsimile Catalog Cards for Laboratory Technical Publications, a facsimile catalog card in Library of Congress MARC format is reproduced below.

Huval, Carl John
Savannah Harbor investigation and model study; Volume IV: Reanalysis of freshwater control plan; numerical model study / by Carl J. Huval ... [et al.]. Vicksburg, Miss. U. S. Waterways Experiment Station ; Springfield, Va. : available from National Technical Information Service, 1979.
17, [24] p., 16 leaves of plates : ill. ; 27 cm. (Technical report - U. S. Army Engineer Waterways Experiment Station ; 2-580, v.4)
Prepared for U. S. Army Engineer District, Savannah, Savannah, Georgia.

1. Environmental effects. 2. Fresh water. 3. Mathematical models. 4. Salinity. 5. Salt water intrusion. 6. Savannah Harbor. I. United States. Army. Corps of Engineers. Savannah District. II. Series: United States. Waterways Experiment Station, Vicksburg, Miss. Technical report ; 2-580, v.4.
TA7.W34 no.2-580 v.4